normoxia. In contrast, under hypoxia, immunoprecipitation experiment indicated that E2 in the presence of BMP2 caused the binding of p-Smad1/5/8 to ER and HIF-1α in the nucleus. This is consistent with a report by Chun et al in which HIF-1α induced by hypoxia was shown to be localized in the cell nucleus.[31] There is neither a HIF-1α- nor an ER-binding site in the Id1 promoter region, whereas the Smad-binding region is located approximately –1 kb upstream from the Id1 promoter.[22] We propose the following possibilities: (1) the binding complex formed by p-Smad1/5/8, HIF-1α, and ER in the nucleus may inhibit p-Smad1/5/8 binding to the promoter regions of the target genes such as Id1 and decrease BMP signal transduction; or (2) although p-Smad1/5/8 was transported to the nucleus, it might be rapidly exported from there for degradation after formation of the binding complex. Yamamoto et al confirmed the binding of Smad1 with ER in MCF-7 and HEK293 cells.[27] Cho et al reported that ERα downregulation under hypoxia involves protein-protein interactions between ERα and HIF-1α in MCF-7.[32] Masuda et al showed that fibroblast growth factor (FGF) 8 increases the expression levels of estrogen and ER signaling, and inhibits Smad1/5/8 signal activity through suppression of the expression of BMPR2 in MCF-7 cells.[33] Ito et al proposed that ERα forms a protein complex with Smad and induces simultaneous degradation of these proteins through a ubiquitin-proteasome system to inhibit transforming growth factor (TGF) β pathways in an estrogen-dependent manner.[34] Further studies are needed to elucidate the detailed mechanisms underlying the alteration of BMP signaling under normoxia and hypoxia.

Austin et al reported that variations in estrogens and their metabolism could have adverse effects on PAH development with *BMPR2* mutations.[35] White et al reported that female mice overexpressing the serotonin transporter (SERT+ mice) developed PAH, which was abolished by ovariectomy, but male SERT+ mice did not develop PAH. Long-term treatment with E2 progressed the PAH phenotype in ovariectomized female SERT+ mice.[36] Dempsie et al reported that female mice overexpressing the calcium-binding protein S100A4/Mts1 (Mts1+ mice) developed PAH and pulmonary vascular remodeling, whereas male Mts1+ mice remained unaffected. The development of plexiform-like lesions in Mts1+ mice was specific to the female.[37] The aforementioned evidence is consistent with recent findings in human PAH. The present results explain, at least in part, the mechanism by which estrogen exerts contradictory effects in vivo, although the role of gender and/or estrogen in the development of PAH is still controversial.

Conclusion

Estrogen-induced changes in the BMP signaling in HPAEC altered, depending on the expression of HIF-1α, and different mechanisms may be involved in the estrogen effects on BMP signaling. Although further investigations are needed to examine the precise mechanisms involved, these in vitro data indicate that estrogen may act as an adverse factor in PAH development in some instances, which could explain at least in part the reason for the female predominance in idiopathic PAH.

Acknowledgments

We thank Dr K. Iwai (Kyoto University), Dr T. Katagiri (Saitama Medical University), Dr M. Makishima (Nihon University), Dr N. Tsumaki (Kyoto University), and Dr J. Yanagisawa (Tsukuba University) for providing advice and materials.

Disclosures

Name of grant: no financial assistance. Conflict of Interest: none declared.

References

1. Simonneau G, Robbins IM, Beghetti M, Channick RN, Delcroix M, Denton CP, et al. Updated clinical classification of pulmonary hypertension. *J Am Coll Cardiol* 2009; **54:** S43–S54.
2. Fukumoto Y, Shimokawa H. Recent progress in the management of pulmonary hypertension. *Circ J* 2011; **75:** 1801–1810.
3. Chida A, Shintani M, Nakayama T, Furutani Y, Hayama E, Inai K, et al. Missense mutations of the BMPR1B (ALK6) gene in childhood idiopathic pulmonary arterial hypertension. *Circ J* 2012; **76:** 1501–1508.
4. Fujiwara M, Yagi H, Matsuoka R, Akimoto K, Furutani M, Imamura S, et al. Implications of mutations of activin receptor-like kinase 1 gene (ALK1) in addition to bone morphogenetic protein receptor II gene (BMPR2) in children with pulmonary arterial hypertension. *Circ J* 2008; **72:** 127–133.
5. Shintani M, Yagi H, Nakayama T, Saji T, Matsuoka R. A new nonsense mutation of SMAD8 associated with pulmonary arterial hypertension. *J Med Genet* 2009; **46:** 331–337.
6. International PPH Consortium, Lane KB, Machado RD, Pauciulo MW, Thomson JR, Phillips JA 3rd, Loyd JE, et al. Heterozygous germline mutations in BMPR2, encoding a TGF-beta receptor, cause familial primary pulmonary hypertension. *Nat Genet* 2000; **26:** 81–84.
7. Machado RD, Aldred MA, James V, Harrison RE, Patel B, Schwalbe EC, et al. Mutations of the TGF-beta type II receptor BMPR2 in pulmonary arterial hypertension. *Hum Mutat* 2006; **27:** 121–132.
8. Thomson JR, Machado RD, Pauciulo MW, Morgan NV, Humbert M, Elliott GC, et al. Sporadic primary pulmonary hypertension is associated with germline mutations of the gene encoding BMPR-II, a receptor member of the TGF-beta family. *J Med Genet* 2000; **37:** 741–745.
9. Atkinson C, Stewart S, Upton PD, Machado R, Thomson JR, Trembath RC, et al. Primary pulmonary hypertension is associated with reduced pulmonary vascular expression of type II bone morphogenetic protein receptor. *Circulation* 2002; **105:** 1672–1678.
10. Austin ED, Loyd JE, Phillips JA 3rd. Genetics of pulmonary arterial hypertension. *Semin Respir Crit Care Med* 2009; **30:** 386–398.
11. Rosenzweig EB, Morse JH, Knowles JA, Chada KK, Khan AM, Roberts KE, et al. Clinical implications of determining BMPR2 mutation status in a large cohort of children and adults with pulmonary arterial hypertension. *J Heart Lung Transplant* 2008; **27:** 668–674.
12. Beretta L, Caronni M, Origgi L, Ponti A, Santaniello A, Scorza R. Hormone replacement therapy may prevent the development of isolated pulmonary hypertension in patients with systemic sclerosis and limited cutaneous involvement. *Scand J Rheumatol* 2006; **35:** 468–471.
13. Lahm T, Crisostomo PR, Markel TA, Wang M, Weil BR, Novotny NM, et al. The effects of estrogen on pulmonary artery vasoreactivity and hypoxic pulmonary vasoconstriction: Potential new clinical implications for an old hormone. *Crit Care Med* 2008; **36:** 2174–2183.
14. Miyazono K, Kamiya Y, Morikawa M. Bone morphogenetic protein receptors and signal transduction. *J Biochem* 2010; **147:** 35–51.
15. Takahashi K, Kogaki S, Matsushita T, Nasuno S, Kurotobi S, Ozono K. Hypoxia induces alteration of bone morphogenetic protein receptor signaling in pulmonary artery endothelial cell. *Pediatr Res* 2007; **61:** 392–397.
16. Richter A, Yeager ME, Zaiman A, Cool CD, Voelkel NF, Tuder RM. Impaired transforming growth factor-beta signaling in idiopathic pulmonary arterial hypertension. *Am J Respir Crit Care Med* 2004; **170:** 1340–1348.
17. Cool CD, Stewart JS, Werahera P, Miller GJ, Williams RL, Voelkel NF, et al. Three-dimensional reconstruction of pulmonary arteries in plexiform pulmonary hypertension using cell-specific markers: Evidence for a dynamic and heterogeneous process of pulmonary endothelial cell growth. *Am J Pathol* 1999; **155:** 411–419.
18. Morty RE, Nejman B, Kwapiszewska G, Hecker M, Zakrzewicz A, Kouri FM, et al. Dysregulated bone morphogenetic protein signaling in monocrotaline-induced pulmonary arterial hypertension. *Arterioscler Thromb Vasc Biol* 2007; **27:** 1072–1078.
19. Tuder RM, Chacon M, Alger L, Wang J, Taraseviciene-Stewart L, Kasahara Y, et al. Expression of angiogenesis-related molecules in plexiform lesions in severe pulmonary hypertension: Evidence for a process of disordered angiogenesis. *J Pathol* 2001; **195:** 367–374.
20. Hiraga T, Kizaka-Kondoh S, Hirota K, Hiraoka M, Yoneda T. Hypoxia and hypoxia-inducible factor-1 expression enhance osteolytic bone metastases of breast cancer. *Cancer Res* 2007; **67:** 4157–4163.
21. Kelly BD, Hackett SF, Hirota K, Oshima Y, Cai Z, Berg-Dixon S, et

al. Cell type-specific regulation of angiogenic growth factor gene expression and induction of angiogenesis in nonischemic tissue by a constitutively active form of hypoxia-inducible factor 1. *Circ Res* 2003; **93:** 1074–1081.
22. Katagiri T, Imada M, Yanai T, Suda T, Takahashi N, Kamijo R. Identification of a BMP-responsive element in Id1, the gene for inhibition of myogenesis. *Genes Cells* 2002; **7:** 949–960.
23. Janowski BA, Willy PJ, Devi TR, Falck JR, Mangelsdorf DJ. An oxysterol signalling pathway mediated by the nuclear receptor LXR alpha. *Nature* 1996; **383:** 728–731.
24. Kawai M, Namba N, Mushiake S, Etani Y, Nishimura R, Makishima M, et al. Growth hormone stimulates adipogenesis of 3T3-L1 cells through activation of the Stat5A/5B-PPARgamma pathway. *J Mol Endocrinol* 2007; **38:** 19–34.
25. Rubin LJ. Primary pulmonary hypertension. *N Engl J Med* 1997; **336:** 111–117.
26. Humbert M, Morrell NW, Archer SL, Stenmark KR, MacLean MR, Lang IM, et al. Cellular and molecular pathobiology of pulmonary arterial hypertension. *J Am Coll Cardiol* 2004; **43:** 13S–24S.
27. Yamamoto T, Saatcioglu F, Matsuda T. Cross-talk between bone morphogenic proteins and estrogen receptor signaling. *Endocrinology* 2002; **143:** 2635–2642.
28. Paez-Pereda M, Giacomini D, Refojo D, Nagashima AC, Hopfner U, Grubler Y, et al. Involvement of bone morphogenetic protein 4 (BMP-4) in pituitary prolactinoma pathogenesis through a Smad/estrogen receptor crosstalk. *Proc Natl Acad Sci USA* 2003; **100:** 1034–1039.
29. Helms MW, Packeisen J, August C, Schittek B, Boecker W, Brandt BH, et al. First evidence supporting a potential role for the BMP/SMAD pathway in the progression of oestrogen receptor-positive breast cancer. *J Pathol* 2005; **206:** 366–376.
30. Fijalkowska I, Xu W, Comhair SA, Janocha AM, Mavrakis LA, Krishnamachary B, et al. Hypoxia inducible-factor1alpha regulates the metabolic shift of pulmonary hypertensive endothelial cells. *Am J Pathol* 2010; **176:** 1130–1138.
31. Chun YS, Choi E, Yeo EJ, Lee JH, Kim MS, Park JW. A new HIF-1 alpha variant induced by zinc ion suppresses HIF-1-mediated hypoxic responses. *J Cell Sci* 2001; **114:** 4051–4061.
32. Cho J, Kim D, Lee S, Lee Y. Cobalt chloride-induced estrogen receptor alpha down-regulation involves hypoxia-inducible factor-1alpha in MCF-7 human breast cancer cells. *Mol Endocrinol* 2005; **19:** 1191–1199.
33. Masuda H, Otsuka F, Matsumoto Y, Takano M, Miyoshi T, Inagaki K, et al. Functional interaction of fibroblast growth factor-8, bone morphogenetic protein and estrogen receptor in breast cancer cell proliferation. *Mol Cell Endocrinol* 2011; **343:** 7–17.
34. Ito I, Hanyu A, Wayama M, Goto N, Katsuno Y, Kawasaki S, et al. Estrogen inhibits transforming growth factor beta signaling by promoting Smad2/3 degradation. *J Biol Chem* 2010; **285:** 14747–14755.
35. Austin ED, Cogan JD, West JD, Hedges LK, Hamid R, Dawson EP, et al. Alterations in oestrogen metabolism: Implications for higher penetrance of familial pulmonary arterial hypertension in females. *Eur Respir J* 2009; **34:** 1093–1099.
36. White K, Dempsie Y, Nilsen M, Wright AF, Loughlin L, MacLean MR. The serotonin transporter, gender, and 17beta oestradiol in the development of pulmonary arterial hypertension. *Cardiovasc Res* 2011; **90:** 373–382.
37. Dempsie Y, Nilsen M, White K, Mair KM, Loughlin L, Ambartsumian N, et al. Development of pulmonary arterial hypertension in mice over-expressing S100A4/Mts1 is specific to females. *Respir Res* 2011; **12:** 159.

Bone 56 (2013) 375–382

Contents lists available at ScienceDirect

Bone

journal homepage: www.elsevier.com/locate/bone

Original Full Length Article

A human skeletal overgrowth mutation increases maximal velocity and blocks desensitization of guanylyl cyclase-B ☆

Jerid W. Robinson [a,1], Deborah M. Dickey [b,1], Kohji Miura [c], Toshimi Michigami [d], Keiichi Ozono [c], Lincoln R. Potter [a,b,*]

[a] Department of Pharmacology, University of Minnesota, Minneapolis, MN, USA
[b] Department of Biochemistry, Molecular Biology and Biophysics, University of Minnesota, Minneapolis, MN, USA
[c] Department of Pediatrics, Osaka Graduate School of Medicine, Osaka, Japan
[d] Department of Bone and Mineral Research, Osaka Medical Center and Research Institute for Maternal and Child Health, Osaka, Japan

ARTICLE INFO

Article history:
Received 18 February 2013
Revised 12 June 2013
Accepted 24 June 2013
Available online 1 July 2013

Edited by: R. Baron

Keywords:
Natriuretic peptides
Guanylate cyclase
Bone growth
cGMP
Dwarfism
Achondroplasia

ABSTRACT

C-type natriuretic peptide (CNP) increases long bone growth by stimulating guanylyl cyclase (GC)-B/NPR-B/NPR2. Recently, a Val to Met missense mutation at position 883 in the catalytic domain of GC-B was identified in humans with increased blood cGMP levels that cause abnormally long bones. Here, we determined how this mutation activates GC-B. In the absence of CNP, cGMP levels in cells expressing V883M-GC-B were increased more than 20 fold compared to cells expressing wild-type (WT)-GC-B, and the addition of CNP only further increased cGMP levels 2-fold. In the absence of CNP, maximal enzymatic activity (Vmax) of V883M-GC-B was increased 15-fold compared to WT-GC-B but the affinity of the enzymes for substrate as revealed by the Michaelis constant (Km) was unaffected. Surprisingly, CNP decreased the Km of V883M-GC-B 10-fold in a concentration-dependent manner without increasing Vmax. Unlike the WT enzyme the Km reduction of V883M-GC-B did not require ATP. Unexpectedly, V883M-GC-B, but not WT-GC-B, failed to inactivate with time. Phosphorylation elevated but was not required for the activity increase associated with the mutation because the Val to Met substitution also activated a GC-B mutant lacking all known phosphorylation sites. We conclude that the V883M mutation increases maximal velocity in the absence of CNP, eliminates the requirement for ATP in the CNP-dependent Km reduction, and disrupts the normal inactivation process.

Introduction

C-type natriuretic peptide (CNP) stimulates long bone growth and inhibits meiotic resumption in oocytes by activating the enzyme variously known as guanylyl cyclase (GC)-B, natriuretic peptide receptor (NPR)-2 or NPR-B, which catalyzes the synthesis of the intracellular signaling molecule, cGMP [1–3]. GC-B is a homodimer containing an extracellular ligand-binding domain, a single membrane-spanning region, and an intracellular highly phosphorylated kinase homology domain, dimerization domain and C-terminal GC catalytic domain [4].

CNP binding increases GC-B activity by two mechanisms. It increases the maximal rate of cGMP production called maximal velocity (Vmax) and it also increases the affinity of the enzyme for GTP that is observed as a reduction in the Michaelis constant — the GTP concentration required to reach half the Vmax. Under non-physiologic conditions such as an enzyme assay where ATP is not present, the activity of GC-B is positive cooperative as demonstrated by a Hill coefficient of greater than 1. This means that GTP binds an allosteric site that increases the affinity of the catalytic site for GTP. However, under biological conditions where ATP concentrations are at or above 1 mM, the Hill coefficient of GC-B is 1 because the allosteric site is occupied by ATP not GTP. Recently, we demonstrated that ATP is required for the CNP-dependent reduction in the Km of GC-B [5,6]. Finally, in broken cell assays, ATP also increases GC-B activity by providing the phosphate that is added to the serine and threonine residues on the enzyme that is necessary for activation by CNP [7,8].

GC-B was identified in rat chondrocytes in 1994 [9], but the ability of natriuretic peptides to stimulate skeletal growth was first observed in transgenic mice overexpressing BNP in 1998 [10]. Subsequent bone culture studies indicated that CNP, not BNP, increased the proliferative and hypertrophic zones of the murine growth plate, which increases the length of long bones [10]. CNP also increases the earliest stage of endochondral bone development – the condensation of mesenchymal precursor cells – as well as stimulates glycosaminoglycan synthesis and extracellular matrix production [11,12]. Consistent with the requirement of CNP and GC-B in normal long bone growth in mammals, mice lacking either CNP or GC-B were dwarfs [13,14], and mice lacking the

Abbreviations: CNP, C-type natriuretic peptide; GC, guanylyl cyclase; NP, natriuretic peptide; WT, wild type.

☆ Disclosure statement: The authors have nothing to declare.

* Corresponding author at: University of Minnesota — Twin Cities, 6-155 Jackson Hall, 321 Church St. SE, Minneapolis, MN 55455, USA. Fax: +1 612 624 7282.
E-mail address: potter@umn.edu (L.R. Potter).

[1] Contributed equally to this manuscript and should be considered co-first authors.

8756-3282/$ – see front matter © 2013 Elsevier Inc. All rights reserved.
http://dx.doi.org/10.1016/j.bone.2013.06.024

natriuretic peptide clearance receptor (NPR-C) that degrades CNP exhibited skeletal hyperplasia [15,16]. In contrast, mice lacking BNP display no skeletal abnormalities [17]. Importantly, CNP and CNP analogs were recently shown to increase long bone growth in murine models of achondroplasia [18–20].

Homozygous inactivating mutations in both alleles of GC-B were identified in humans with acromesomelic dysplasia, type Maroteaux (AMDM) dwarfism [21–23], and heterozygous mutations in GC-B were associated with non-pathological reductions in human stature [24]. Conversely, mutations associated with CNP overexpression were identified in patients with skeletal overgrowth [25,26], and a genome-wide association study identified correlations between genetic mutations that regulate CNP or NPR-C expression and height in Northwestern European populations [27].

In 2012, Miura et al. identified a conserved valine to methionine missense mutation at position 883 in the catalytic domain of human GC-B (V883M-GC-B) in three generations of a Japanese family with skeletal overgrowth, fragile bones and elevated blood cGMP concentrations [28]. Importantly, how this mutation increases GC-B activity was not determined. Here, we show that this single residue substitution increases the maximal velocity of GC-B in the absence of CNP and that CNP reduces the Km of V883M-GC-B an order of magnitude without ATP or without increasing maximal velocity. Unexpectedly, the V883M substitution blocked the normal inactivation process.

Materials and methods

Reagents

^{125}I-cGMP radioimmunoassay kits and ^{32}P-α-GTP were from Perkin Elmer (Waltham, MA). CNP-22 was purchased from Sigma (St. Louis, MO). The plasmids encoding the N-terminally HA-tagged form of WT human GC-B (HA-WT-GC-B) [22] and HA-V883M-GC-B plasmids [28] have been described. The plasmids expressing rat GC-B-7A and GC-B-7E were also previously described [29,30]. The ATDC5 chondrocytes were from ATCC (www.atcc.org).

Cells and transfections

293 neocells were maintained and transiently transfected by the HEPES–calcium-phosphate precipitation method as previously reported [30].

Whole cell cGMP elevation assays

Cyclic GMP concentrations were measured by radioimmunoassay in ethanol extracts of transiently transfected 293 cells that were pre-incubated with 1 mM isobutylmethyl xanthine, a general phosphodiesterase inhibitor, for 10 min before being incubated with increasing concentrations of CNP as previously described [31].

Guanylyl cyclase assays

Crude membranes were prepared at 4 °C in phosphatase inhibitor buffer consisting of 50 mM 4-(2-hydroxyethyl)-1-piperazineethanesulfonic acid — pH 7.4, 50 mM NaCl, 20% glycerol, 50 mM NaF, 1 mM EDTA, 0.5 μM microcystin and 1× Roche protease inhibitor cocktail. All assays were performed at 37 °C in a cocktail containing 25 mM HEPES pH 7.4, 50 mM NaCl, 0.1% BSA, 0.5 mM isobutylmethyl xanthine, 1 mM EDTA, 0.5 μM microcystin, 5 mM phosphocreatine, 0.1 μg/μl creatine kinase and 5 mM $MgCl_2$.

The single substrate concentration GC assays were performed using ^{32}P-GTP as substrate in the presence of 1 mM ATP and 1 mM GTP at 37 °C for 3 min as previously described [31]. For the desensitization assays, the reaction was performed using a pool of crude membranes. The reaction was initiated by the addition of pre-warmed cocktail. At the designated times, 0.1 ml aliquots were removed and added to ice-cold tubes containing 0.5 ml zinc acetate to stop the reaction. Alumina column chromatography purified the ^{32}P-cGMP, which was quantified by Cerenkov counting [32].

Substrate-velocity assays were performed for the indicated times with the indicated GTP concentrations. The resulting cGMP concentrations were determined by radioimmunoassay as described [33]. When included, free manganese concentrations in the assays were 2 mM. Because enzymatic activity was not completely linear with time, the kinetic parameters obtained under these conditions are considered "apparent".

Western blotting

293T cells were transfected with the indicated constructs, immunoprecipitated, fractionated by reducing SDS-PAGE and blotted to an Immobilon membrane for immune-detection as previously described [34]. The blot was blocked and probed with at 1/2500 dilution of rabbit serum 6328 followed by incubation with a 1/20,000 dilution of goat anti-rabbit IRDye 680 conjugated antibody and visualized on a LI-COR instrument as previously described [35].

Statistical analysis

Statistics and graphs were generated with Prism 5 software. Student's paired *t*-test determined significance where $p \leq 0.05$ was considered significant. The vertical bars within the symbols represent the SEM. Where not visible the bars are contained within the symbol. EC_{50} values were calculated based on the nonlinear curve fitting equation $Y = Top * X / (EC_{50} + X)$. Substrate–velocity curves were analyzed using an allosteric sigmoidal model to generate Hill coefficients.

Results

Cyclic GMP is elevated more than twenty-fold in cells expressing GC-B-V883M

HEK293 cells were transiently transfected with human isoforms of HA-WT-GC-B or HA-V883M-GC-B. Two days later, the cells were incubated in the presence of increasing concentrations of CNP for 3 min and intracellular cGMP concentrations were determined (Fig. 1A). Basal (no CNP) cGMP concentrations were elevated 21-fold in cells expressing HA-V883M-GC-B compared to cells expressing HA-WT-GC-B. Maximal concentrations of CNP increased cGMP concentrations 29-fold in HA-WT-GC-B expressing cells but only 2-fold in cells expressing HA-V883M-GC-B. The EC_{50} for CNP activation was not significantly different between the WT and mutant enzymes, consistent with the mutation not affecting the affinity of CNP for GC-B.

Plasmids expressing WT and GC-B-V883M were also transiently transfected into ATDC5 mouse chondrocytic cells that endogenously express GC-B. Since these cells express phosphodiesterases 1 and 5, we pretreated them with a general phosphodiesterase to emphasize cGMP synthesis by GC-B [36]. Overexpression of WT-GC-B slightly elevated cyclic GMP concentrations in the ATDC5 cells, but overexpression of the GC-B-V883M mutant resulted in cGMP levels that were more than four-fold higher than those observed in cells transfected with the WT enzyme (Fig. 1B). These data indicate that the increased basal activity associated with the V883M mutation occurs in a natural cellular environment for GC-B and is consistent with the increased plasma cGMP concentrations measured in patients expressing V883M-GC-B [28].

Basal enzymatic activity of V883M-GC-B is elevated but expression is reduced

GC activity was measured in crude membranes from 293 cells expressing green fluorescent protein (GFP) as a control, WT-GC-B,

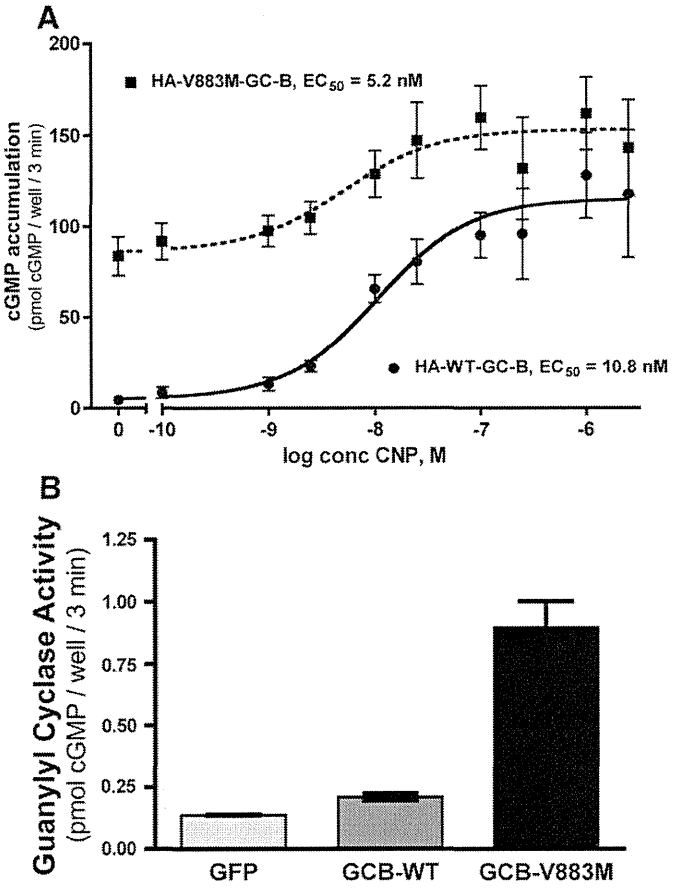

Fig. 1. Basal cGMP concentrations are markedly elevated in cells expressing V883M-GC-B. A, 293 cells transiently expressing HA-WT-GC-B or HA-V883M-GC-B were incubated with the indicated concentrations of CNP for 3 min and then intracellular cGMP concentrations were determined. The EC_{50}s for the two enzymes were not significantly different, $p = 0.42$. B, ATDC5 cells were transiently transfected with plasmids expressing WT-GC-B or GC-B-V883M and cGMP concentrations were measured in basal (no CNP) serum-starved cells 2 days later. Cyclic GMP concentrations in cells expressing WT-GC-B were slightly higher than those observed in un-transfected cells ($p < 0.01$), but levels in cells expressing GC-B-V883M were 4.3-fold higher than those in cells expressing WT-GC-B ($p < 0.03$).

HA-WT-GC-B or HA-V883M-GC-B under basal (1 mM Mg^{2+}GTP), hormone-stimulated (1 mM Mg^{2+}GTP, 1 mM ATP and 1 μM CNP), or detergent-stimulated (1 mM Mn^{2+}GTP and 1% Triton X-100) condition (Fig. 2). Enzyme analysis was performed in the 293 cells because they do not express detectable endogenous GC activity [6], which allows more definitive interpretation of the data because most tissues and cell lines express more than one GC.

GC activity measured in crude membranes from GFP transfected cells was insignificant under all conditions. Consistent with the whole cell cGMP analysis describe in Fig. 1, basal GC activity was low for WT-GC-B and HA-WT-GC-B but was elevated 28-fold over WT levels for HA-V883M-GC-B. Saturating concentrations of CNP and ATP stimulated WT-GC-B and HA-WT-GC-B similarly (>50-fold). However, GC activity of HA-WT-GC-B was almost double that of the WT enzyme lacking the HA tag, consistent with higher expression of the HA-tagged receptor. As in whole cells, CNP and ATP activated HA-V883M-GC-B about two-fold in enzyme assays. GC activity of HA-V883M-GC-B measured in the presence of detergent was lower than that observed for HA-WT-GC-B, which is consistent with reduced expression of HA-V883M-GC-B compared to HA-WT-GC-B. Western analysis of SDS-PAGE fractionated immunoprecipitated enzymes confirmed that the more slowly migrating, completely processed species (upper band) was expressed at lower levels than the comparably processed forms of the tagged or untagged WT version of GC-B (Fig. 2, inset). We previously

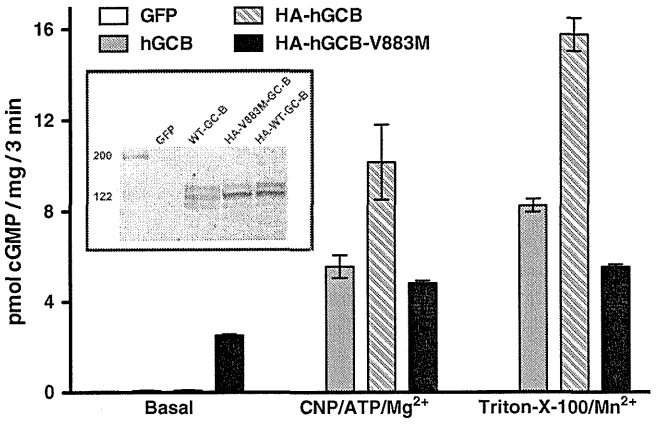

Fig. 2. GC activity but not the protein level of V883M-GC-B was elevated in the absence of CNP. Crude membranes from 293 cells transfected with plasmids expressing the indicated constructs were assayed for GC activity under the conditions indicated in the figure legend and text. Bars within the symbols indicate the range of duplicate determinations. This figure is representative of two independent assays. The inset shows a Western blot of the indicated forms of GC-B purified from 293 cells transiently transfected with the indicated constructs. The numbers on the left indicate the molecular weight of standards.

demonstrated that only the upper band of GC-B is phosphorylated and that phosphorylation is required for CNP-dependent activation of GC-B [8,29].

Maximal velocity of HA-GC-B-V883M is elevated

To determine how the mutation increased the enzymatic activity of GC-B, substrate–velocity curves were generated for HA-WT-GC-B and HA-V883M-GC-B with or without 1 μM CNP in the absence of ATP (Fig. 3A). Basal activity of the WT enzyme was low and CNP increased Vmax 12-fold without decreasing the Km. Consistent with previous observations [6], WT-GC-B was positive cooperative as indicated by a Hill slope of 1.3. In contrast, basal maximal velocity of the mutant enzyme was elevated 15-fold compared to WT-GC-B and the Km was unchanged. The Hill coefficient was 0.9, suggesting slight negative cooperativity. CNP failed to increase the maximal velocity of HA-V883M-GC-B, but reduced the Hill slope 0.4 units and the Km 10-fold. Thus, the V883M mutation increases basal maximal velocity, reduces the Hill coefficient and allows CNP to reduce the Km in the absence of ATP. In contrast, the reduction in Hill coefficient and Km for the WT enzyme was previously shown to be completely dependent on the presence of ATP [5]. These data are consistent with the V883M mutation producing a structural change in GC-B that locks it into a conformation that mimics that of the ATP-bound state. They also indicate for the first time that the CNP-dependent changes in the Vmax and Km of GC-B are separate but related processes.

CNP reduces the Hill coefficient and Km of HA-V883M-GC-B in a concentration-dependent manner in the absence of ATP

Substrate–velocity curves were generated for HA-V883M-GC-B in the presence of increasing concentrations of CNP to evaluate the concentration-dependence of CNP on reductions in the Hill coefficient and Michaelis constant (Fig. 3B). ATP was not included in these experiments. In the absence of CNP, no cooperativity was observed, but increasing concentrations of CNP progressively increased the amount of negative cooperativity while concomitantly decreasing the Km. These data indicate that CNP converts HA-V883M-GC-B to a strongly negative cooperative enzyme. Similarly, in the absence of CNP, the Km of the mutant enzyme was high; but in the presence of increasing concentrations of CNP, the Km dropped progressively while maximal velocity was unaffected.

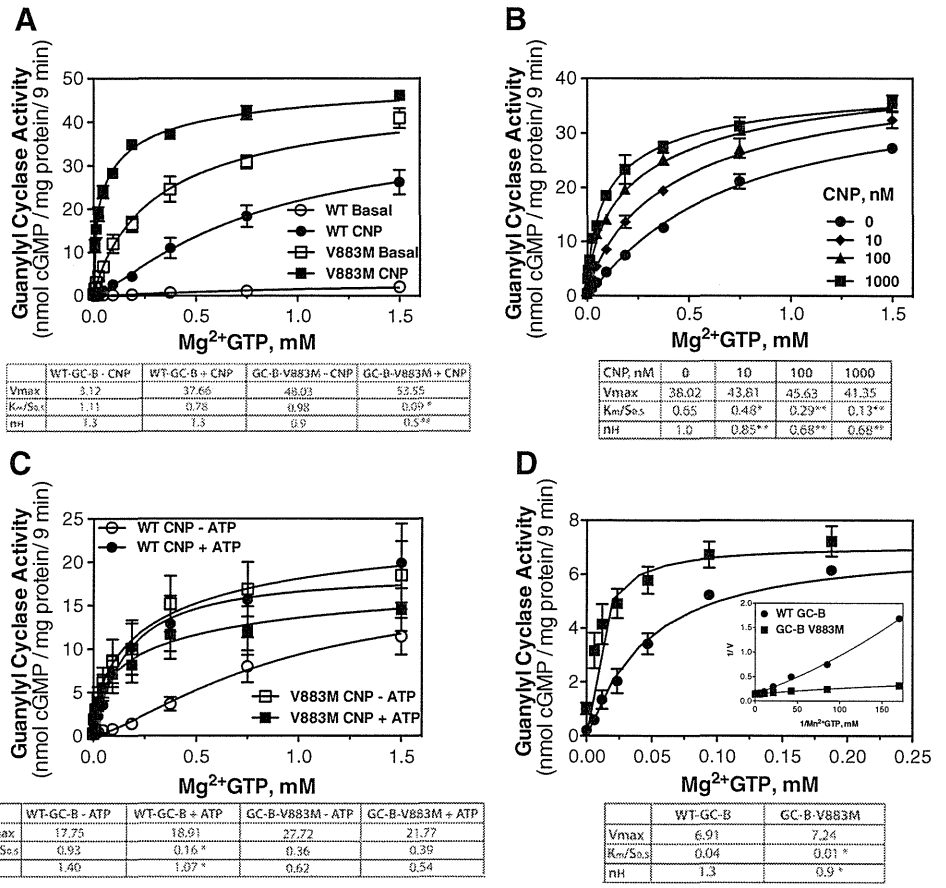

	WT-GC-B - CNP	WT-GC-B + CNP	GC-B-V883M - CNP	GC-B-V883M + CNP
Vmax	3.12	37.66	48.03	53.55
Km/So.5	1.11	0.78	0.98	0.69 *
nH	1.3	1.3	0.9	0.5**

CNP, nM	0	10	100	1000
Vmax	38.02	43.81	45.63	41.35
Km/So.5	0.65	0.48*	0.29**	0.13**
nH	1.0	0.85**	0.68**	0.68**

	WT-GC-B - ATP	WT-GC-B + ATP	GC-B-V883M - ATP	GC-B-V883M + ATP
Vmax	17.75	18.91	27.72	21.77
Km/So.5	0.93	0.16 *	0.36	0.39
nH	1.40	1.07 *	0.62	0.54

	WT-GC-B	GC-B-V883M
Vmax	6.91	7.24
Km/So.5	0.04	0.01 *
nH	1.3	0.9 *

Fig. 3. Kinetic characterization of V883M-GC-B. GC activity shown in panels A–D was measured for 9 min in crude membranes from 293 cells transiently expressing either HA-GC-B-WT or HA-GC-B-V883M. Bars within symbols indicate the SEM. Tables below each figure show Vmax, Km and Hill coefficient (n_H). A. Maximal velocity of HA-V883M-GC-B is elevated in the absence of CNP. GC activity was measured in the presence or absence of 1 μM CNP and the indicated concentrations of Mg^{2+}GTP where n = 4. The # indicates a significant difference from HA-WT-GC-B-CNP at $p < 0.05$. The ## indicates a significant difference from HA-V883M-GC-B-CNP at $p < 0.03$. B. CNP decreases the Hill coefficient and Km for HA-V883M-GC-B in a concentration-dependent manner in the absence of ATP. GC activity was measured in the presence or absence of increasing concentrations of CNP and the indicated concentrations of Mg^{2+}GTP where n = 4. * and ** indicate a significant difference from no CNP values where $p < 0.05$ and 0.01, respectively. C. ATP does not affect the Hill coefficient or Km of HA-V883M-GC-B. GC activity was measured in the presence or absence of 0.1 mM ATP, 1 μM CNP and the indicated concentrations of Mg^{2+}GTP where n = 4. The * indicates a significant difference from HA-WT-GC-B (−) ATP at $p < 0.05$. D. HA-V883M-GC-B is negative cooperative. GC activity was measured with the indicated concentrations of Mn^{2+}GTP and 1% Triton X-100 where n = 6. The * indicates a significant difference from the corresponding value obtained for the WT enzyme at $p < 0.05$; inset. Double reciprocal plots were generated from the raw data to demonstrate a concave upward curve indicative of positive cooperativity or a slightly downward curve indicative of negative cooperativity.

ATP does not allosterically activate V883M-GC-B

We recently determined that CNP reduces the Hill coefficient and Km of WT-GC-B by a process that requires ATP binding to an allosteric site in the catalytic domain [6]. Therefore, we investigated whether the V883M mutation affected these processes as well. Substrate–velocity curves were generated for HA-WT-GC-B and HA-V883M-GC-B in the presence of 1 μM CNP with or without 0.1 mM ATP. With the WT enzyme, ATP reduced the Km 6-fold and the Hill coefficient 0.3 units without affecting the Vmax (Fig. 3C). However, ATP failed to reduce the Km or Hill coefficient or increase the Vmax of HA-V883M-GC-B. These data are consistent with a scenario where the V883M mutation causes a conformational change in GC-B that abolishes the need for ATP in the CNP-dependent reduction in Hill coefficient and Km.

HA-V883M-GC-B is slightly negative cooperative when manganese is used as a cofactor

Substrate–velocity curves were also generated on membranes expressing HA-WT-GC-B or HA-V883M-GC-B under non-physiologic, detergent conditions using manganese-GTP as substrate (Fig. 3D). Substrate–velocity curves generated under these conditions were previously shown to be positive cooperative for GC-A [37]. Vmax was lower when measured under these conditions but the Km/S0.5 was strikingly lower compared to physiologic activation conditions. Maximal velocity was not different between the WT and mutant GC-B enzymes. The substrate–velocity curve for HA-WT-GC-B was positive cooperative as demonstrated by concave upward reciprocal plots and a Hill coefficient of 1.3 (Fig. 3D, inset). To our knowledge, this is the first demonstration of positive cooperativity for GC-B when assayed under detergent-stimulated conditions. In contrast to HA-WT-GC-B, HA-V883M-GC-B was weakly negative cooperative as indicated by a slightly concave downward curve and a Hill coefficient of 0.9 (Fig. 3D, inset), which is consistent with the slight negative cooperativity observed for V883-GC-B when assayed under basal conditions.

HA-V883M-GC-B is resistant to desensitization

Cyclic GMP concentrations in cells expressing V883M-GC-B were highly elevated two days after transfection (Fig. 1), which suggests that the mutant enzyme was not completely desensitized or downregulated. In contrast, CNP activated WT-GC-B was shown to desensitize in less than one hour [8]. Therefore, we examined whether the V883M mutation disrupted the inactivation of GC-B.

GC activity was measured on membranes from cells expressing HA-WT-GC-B or HA-V883M-GC-B for up to 2 h to evaluate the effect of the V883M mutation on the inactivation of GC-B as a function of time (Fig. 4, top panel). WT GC activity was determined in the

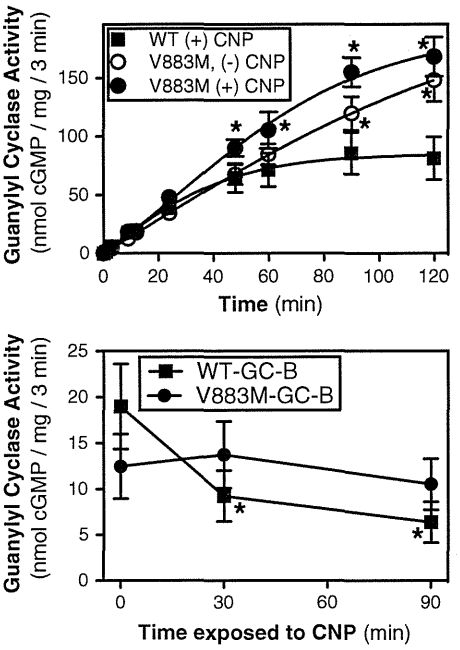

Fig. 4. V883M-GC-B is resistant to desensitization. A. GC assays were conducted on crude membranes from 293 cells transfected with HA-WT-GC-B or HA-V883M-GC-B for the period of time indicated in the presence of 1 mM GTP, 1 mM ATP and 5 mM $Mg^{2+}Cl_2$ with or without 1 μM CNP. Each value represents 4 determinations. The asterisks indicate a significant difference from corresponding values obtained in membranes expressing WT-GC-B at $p < 0.02$. B. Whole 293 cells transfected with HA-WT-GC-B or HA-V883M-GC-B were incubated with 1 μM CNP for the indicated times. Membranes were then prepared and assayed for GC activity in the presence of 1 mM GTP, 1 mM ATP and 5 mM $Mg^{2+}Cl_2$. N = 4. The asterisks indicate significance from the 0 time point value where $p < 0.05$. The bars within the symbols indicate SEM in all panels.

presence of CNP, whereas mutant activity was determined in the presence and absence of CNP. The GC activity of the WT enzyme declined with time and was inactive after 60 min. In contrast, the GC activity of the mutant receptor was linear for the duration of the assay regardless of whether CNP was included in the assay.

We also examined the inactivation of the WT and mutant enzymes under whole cell conditions. In this experiment, intact cells were treated with 1 μM CNP for 0, 30 or 90 min then membranes were prepared from the cells and assayed for GC activity for 3 min (Fig. 4, bottom panel). The WT enzyme demonstrated a time-dependent inactivation similar to that previously reported for GC-B expressed in 3T3 cells [8]. However, exposure of the V883M-GC-B to saturating concentrations of CNP failed to inactivate the enzyme after 30 or 90 min. Together, these data indicate that the Val substitution at position 883 not only increases the maximal velocity of the enzyme, it also disrupts the normal desensitization process.

Activation of GC-B by the V883M substitution does not require phosphorylation

CNP only activated a GC-B construct containing alanine substitutions for the first six phosphorylation sites identified in GC-B (S513, T516, S518, S523, S526, T529) two-fold as opposed to greater than 30-fold for WT-GC-B [29], whereas the analogous substitutions left GC-A completely unresponsive to NP stimulation [38]. These observations led to the idea that phosphorylation is required for NP-dependent activation of GC-A and GC-B. Here, we asked whether phosphorylation is also required for the V883M mutation to increase GC-B activity.

To do this, we mutated Val-883 to Met in the rat GC-B-7A construct that contains alanine substitutions for the first six identified sites plus Ser-522, which is not phosphorylated [29]. We also created a constitutively phosphorylated mimetic version of rat GC-B-V883M by mutating Val-883 to Met in GC-B-7E. Rat GC-B-7E contains glutamate substitutions for the first six identified sites as well as Ser-489, a newly identified putative site that reduces the Km of GC-B when phosphorylated [30].

Introducing the Val-883–Met mutation into WT-GC-B increased basal activity 39-fold, whereas the same mutation in the dephosphorylated form of the enzyme (GC-B-7A) increased activity 17-fold (Fig. 5). However, introduction of the V883M mutation into the GC-B-7E construct increased activity 68-fold. Thus, phosphorylation is not required for the elevated basal activity associated with the V883M mutation, but phosphorylation results in greater activation since the WT and phosphorylation mimetic enzymes (GC-B-7E) were activated to a greater degree than the non-phosphorylated enzyme (GC-B-7A).

Discussion

Characterization of the missense mutant revealed several important changes in GC-B that occurred as a result of this single amino acid substitution. First, basal maximal velocity was dramatically increased. Second, the CNP-dependent reduction in Km was rendered independent of ATP, and thirdly, the normal desensitization process was inactivated. Another worthy point of discussion is that the V883M-GC-B mutant is the first example of a GC where ligand binding reduces the Km without increasing maximal velocity. Thus, the kinetic analysis of this mutant allowed the separation of the maximal velocity increasing effects of ligand binding from the Km reducing effects of ligand binding for the first time. This mutant enzyme also provides unequivocal support for the new GC-B activation model where CNP binding increases activity by reducing the Km as well as increasing maximal velocity [6].

Early studies indicated that product formation by membrane GCs in the presence of detergent is positive cooperative [39,40]. We found that GC-B is positive cooperative under basal conditions as well as when assayed in the presence of Mn^{2+}GTP and Triton X-100. However, the single V883M mutation converts the enzyme from positive cooperative to slightly negative cooperative when assayed under both physiologic and detergent-activated conditions. Interestingly, CNP increased the degree of negative cooperativity of V883M-GC-B in a concentration-dependent manner.

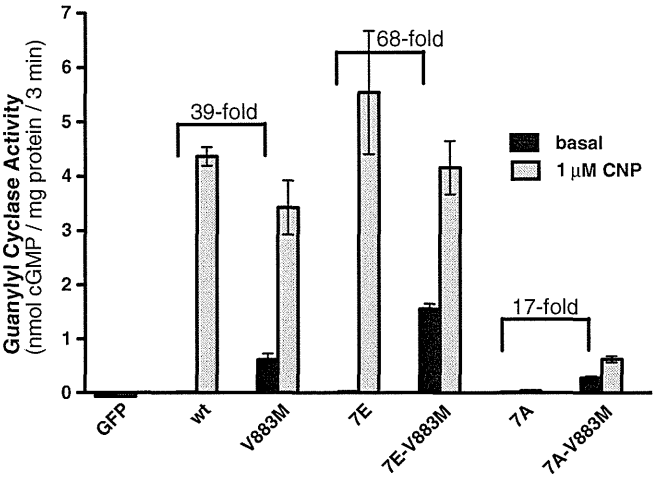

Fig. 5. The GC-B-V883M mutation activates a dephosphorylated version of GC-B. The V883M mutation was introduced into WT-GC-B, constitutively phosphorylated (7E) or constitutively dephosphorylated (7A) forms of GC-B. 293 cells were transiently transfected with plasmids expressing the indicated GC-B constructs. GC assays were performed for 3 min in the presence of 0.1 mM GTP, 1 mM ATP and 5 mM $Mg^{2+}Cl_2$ with or without 1 μM CNP. Each value represents 6 determinations. The bars within the symbols indicate SEM. The values above the brackets indicate the fold-difference above basal values.

The reduction in Km and increase in negative cooperativity appear paradoxical. We hypothesize that the V883M mutant locks the enzyme into a conformation that mimics an ATP bound state. This hypothesis is supported by low or no cooperativity under basal conditions and the inability of ATP to change the activity of the mutant enzyme. In addition, CNP alone markedly decreased the Km of GC-B-V883M, a phenomenon that requires ATP with the WT enzyme. Since cooperativity is maintained, this suggests that the mutation does not destroy the ability of GTP to bind to the allosteric site but rather modifies how GTP binding to the allosteric site affects the catalytic site. However, an alternative

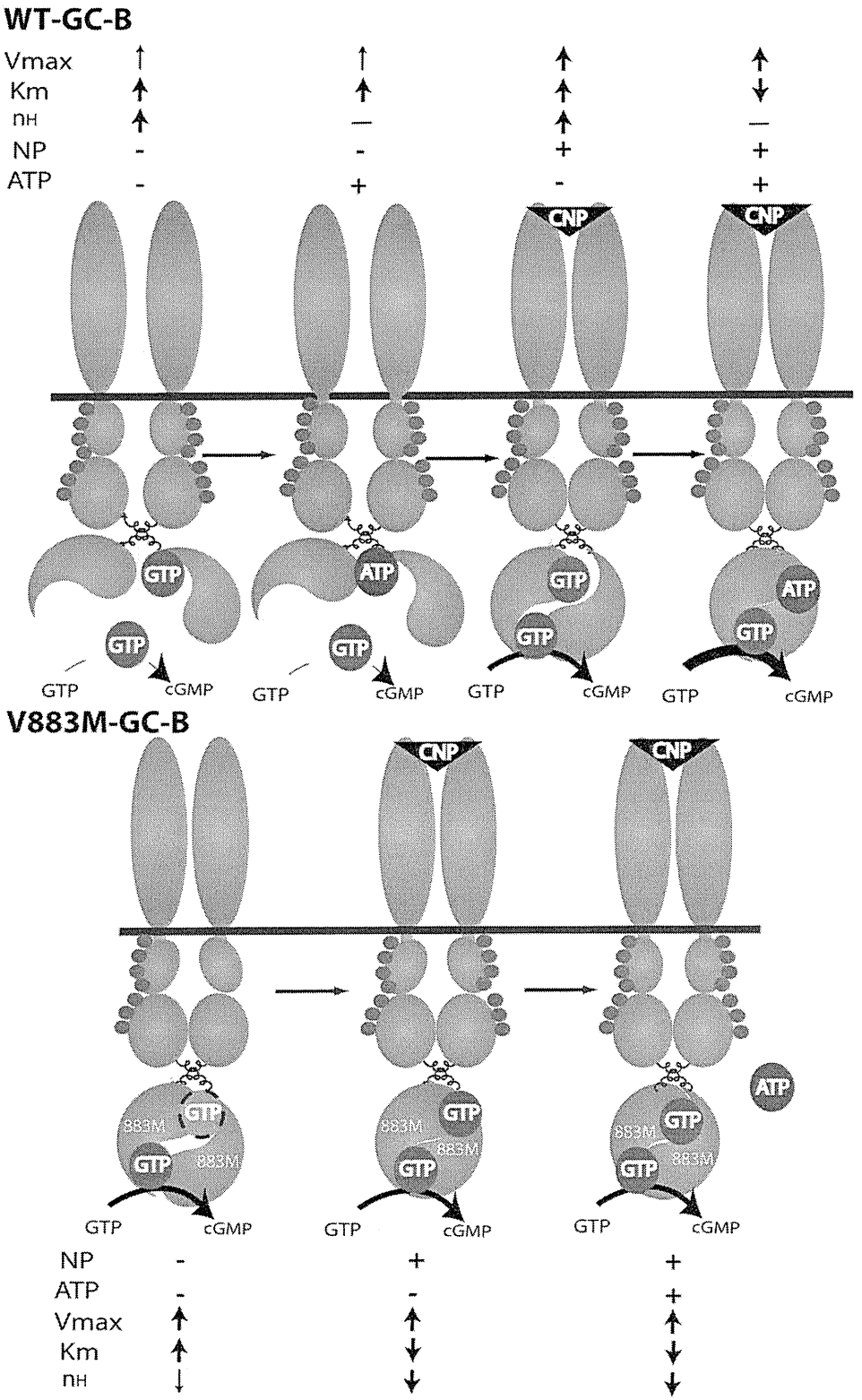

Fig. 6. Activation models for wild type and mutant GC-B. The models are described in detail under the Discussion section. The blue spheres indicate known phosphorylation sites in the kinase homology domain of GC-B. The white 883M indicates that the Val to Met mutation is in the catalytic domain. The abbreviations are: CNP, C-type natriuretic peptide; Km, Michaelis constant; n_H, Hill coefficient; and Vmax, maximal velocity.

explanation is that the reduction in the Hill coefficient results from increased inhibition resulting from GTP binding to a site independent of the allosteric site. This third GTP binding site would explain the appearance of negative cooperativity while also allowing for the Km reduction resulting from the previously identified allosteric site. It is also possible that the V883M mutation could increase the affinity of GC-B for the products of the reaction (pyrophosphate and cGMP), which would result in reduced GC activity and apparent negative cooperativity. Importantly, since the V883M mutation did not affect Vmax when measured in the presence of detergent and manganese, it suggests that the mutation modifies the conformation of the active site under physiologic conditions and does not directly interact with the substrate.

Near linear cGMP production with time by HA-V883M-GC-B assayed both in the presence and absence of CNP indicated that HA-V883M-GC-B is resistant to desensitization. Experiments with alanine and glutamate substituted receptors indicated that unlike CNP activation of WT-GC-B, the increased activity observed with the V883M mutation does not require phosphorylation of the kinase homology domain, although activation was greater with the phosphorylated and phosphomimetic enzymes. The lack of dependence on phosphorylation for activity of the mutant enzyme may contribute to its resistance to desensitization.

It is surprising how much the single amino acid substitution changes the regulation of GC-B (Fig. 6). In the absence of CNP and ATP, maximal velocity of WT-GC-B was low, affinity for substrate was low (high Km), and cooperative was significant and positive. In contrast, under the same conditions, maximal velocity of V883M-GC-B was high, affinity for substrate was low, and cooperativity was low and negative. Addition of ATP in the absence of CNP abolished positive cooperativity of the WT enzyme due to ATP replacing GTP at the allosteric site [6], but had no effect on the mutant enzyme under identical conditions. CNP alone increased maximal velocity of the WT enzyme, but it did not decrease the Km in the absence of ATP. In contrast, CNP alone failed to increase maximal velocity of the mutant enzyme but decreased the Km ten-fold in the absence of ATP. Finally, CNP reduced the cooperativity of both enzymes, but the WT enzyme went from positive to no cooperativity, whereas the mutant went from slightly negative cooperative to very negative cooperative.

In conclusion, we established a molecular mechanism for how a single amino acid substitution in GC-B activates the enzyme, which results in abnormally long and fragile human bones. It will be interesting to determine the prevalence of this mutation in humans and other species.

Conflict of interest statement

None of the authors have a conflict of interest associated with this study.

Acknowledgments

Grant-in Aid (21,922) from the University of Minnesota Graduate School to LRP and the National Institute of Arthritis and Musculoskeletal and Skin Diseases Training Grant T32AR050938 to JWR supported this work.

References

[1] Tamura N, Doolittle LK, Hammer RE, Shelton JM, Richardson JA, Garbers DL. Critical roles of the guanylyl cyclase B receptor in endochondral ossification and development of female reproductive organs. Proc Natl Acad Sci U S A 2004;101:17300–5.
[2] Schmidt H, Stonkute A, Juttner R, Schaffer S, Buttgereit J, Feil R, et al. The receptor guanylyl cyclase Npr2 is essential for sensory axon bifurcation within the spinal cord. J Cell Biol 2007;179:331–40.
[3] Zhang M, Su YQ, Sugiura K, Xia G, Eppig JJ. Granulosa cell ligand NPPC and its receptor NPR2 maintain meiotic arrest in mouse oocytes. Science 2010;330:366–9.
[4] Potter LR, Hunter T. Guanylyl cyclase-linked natriuretic peptide receptors: structure and regulation. J Biol Chem 2001;276:6057–60.
[5] Antos LK, Potter LR. Adenine nucleotides decrease the apparent Km of endogenous natriuretic peptide receptors for GTP. Am J Physiol Endocrinol Metab 2007;293:E1756–63.
[6] Robinson JW, Potter LR. Guanylyl cyclases A and B are asymmetric dimers that are allosterically activated by ATP binding to the catalytic domain. Sci Signal 2012;5:ra65.
[7] Duda T, Goraczniak RM, Sitaramayya A, Sharma RK. Cloning and expression of an ATP-regulated human retina C-type natriuretic factor receptor guanylate cyclase. Biochemistry 1993;32:1391–5.
[8] Potter LR. Phosphorylation-dependent regulation of the guanylyl cyclase-linked natriuretic peptide receptor B: dephosphorylation is a mechanism of desensitization. Biochemistry 1998;37:2422–9.
[9] Hagiwara H, Sakaguchi H, Itakura M, Yoshimoto T, Furuya M, Tanaka S, et al. Autocrine regulation of rat chondrocyte proliferation by natriuretic peptide C and its receptor, natriuretic peptide receptor-B. J Biol Chem 1994;269:10729–33.
[10] Suda M, Ogawa Y, Tanaka K, Tamura N, Yasoda A, Takigawa T, et al. Skeletal overgrowth in transgenic mice that overexpress brain natriuretic peptide. Proc Natl Acad Sci U S A 1998;95:2337–42.
[11] Krejci P, Masri B, Fontaine V, Mekikian PB, Weis M, Prats H, et al. Interaction of fibroblast growth factor and C-natriuretic peptide signaling in regulation of chondrocyte proliferation and extracellular matrix homeostasis. J Cell Sci 2005;118:5089–100.
[12] Woods A, Khan S, Beier F. C-type natriuretic peptide regulates cellular condensation and glycosaminoglycan synthesis during chondrogenesis. Endocrinology 2007;148:5030–41.
[13] Chusho H, Tamura N, Ogawa Y, Yasoda A, Suda M, Miyazawa T, et al. Dwarfism and early death in mice lacking C-type natriuretic peptide. Proc Natl Acad Sci U S A 2001;98:4016–21.
[14] Tamura N, Garbers DL. Regulation of the guanylyl cyclase-B receptor by alternative splicing. J Biol Chem 2003;278:48880–9.
[15] Jaubert J, Jaubert F, Martin N, Washburn LL, Lee BK, Eicher EM, et al. Three new allelic mouse mutations that cause skeletal overgrowth involve the natriuretic peptide receptor C gene (Npr3). Proc Natl Acad Sci U S A 1999;96:10278–83.
[16] Matsukawa N, Grzesik WJ, Takahashi N, Pandey KN, Pang S, Yamauchi M, et al. The natriuretic peptide clearance receptor locally modulates the physiological effects of the natriuretic peptide system. Proc Natl Acad Sci U S A 1999;96:7403–8.
[17] Tamura N, Ogawa Y, Chusho H, Nakamura K, Nakao K, Suda M, et al. Cardiac fibrosis in mice lacking brain natriuretic peptide. Proc Natl Acad Sci U S A 2000;97:4239–44.
[18] Kake T, Kitamura H, Adachi Y, Yoshioka T, Watanabe T, Matsushita H, et al. Chronically elevated plasma C-type natriuretic peptide level stimulates skeletal growth in transgenic mice. Am J Physiol Endocrinol Metab 2009;297:E1339–48.
[19] Lorget F, Kaci N, Peng J, Benoist-Lasselin C, Mugniery E, Oppeneer T, et al. Evaluation of the therapeutic potential of a CNP analog in a Fgfr3 mouse model recapitulating achondroplasia. Am J Hum Genet 2012;91:1108–14.
[20] Yasoda A, Kitamura H, Fujii T, Kondo E, Murao N, Miura M, et al. Systemic administration of C-type natriuretic peptide as a novel therapeutic strategy for skeletal dysplasias. Endocrinology 2009;150:3138–44.
[21] Bartels CF, Bukulmez H, Padayatti P, Rhee DK, van Ravenswaaij-Arts C, Pauli RM, et al. Mutations in the transmembrane natriuretic peptide receptor NPR-B impair skeletal growth and cause acromesomelic dysplasia, type Maroteaux. Am J Hum Genet 2004;75:27–34.
[22] Hachiya R, Ohashi Y, Kamei Y, Suganami T, Mochizuki H, Mitsui N, et al. Intact kinase homology domain of natriuretic peptide receptor-B is essential for skeletal development. J Clin Endocrinol Metab 2007;92:4009–14.
[23] Khan S, Hussain Ali R, Abbasi S, Nawaz M, Muhammad N, Ahmad W. Novel mutations in natriuretic peptide receptor-2 gene underlie acromesomelic dysplasia, type Maroteaux. BMC Med Genet 2012;13:44.
[24] Olney RC, Bukulmez H, Bartels CF, Prickett TC, Espiner EA, Potter LR, et al. Heterozygous mutations in natriuretic peptide receptor-B (NPR2) are associated with short stature. J Clin Endocrinol Metab 2006;91:1229–32.
[25] Bocciardi R, Ravazzolo R. C-type natriuretic peptide and overgrowth. Endocr Dev 2009;14:61–6.
[26] Moncla A, Missirian C, Cacciagli P, Balzamo E, Legeai-Mallet L, Jouve JL, et al. A cluster of translocation breakpoints in 2q37 is associated with overexpression of NPPC in patients with a similar overgrowth phenotype. Hum Mutat 2007;12:1183–8.
[27] Estrada K, Krawczak M, Schreiber S, van Duijn K, Stolk L, van Meurs JB, et al. A genome-wide association study of northwestern Europeans involves the C-type natriuretic peptide signaling pathway in the etiology of human height variation. Hum Mol Genet 2009;18:3516–24.
[28] Miura K, Namba N, Fujiwara M, Ohata Y, Ishida H, Kitaoka T, et al. An overgrowth disorder associated with excessive production of cGMP due to a gain-of-function mutation of the natriuretic peptide receptor 2 gene. PLoS One 2012;7:e42180.
[29] Potter LR, Hunter T. Identification and characterization of the major phosphorylation sites of the B-type natriuretic peptide receptor. J Biol Chem 1998;273:15533–9.
[30] Yoder AR, Robinson JW, Dickey DM, Andersland J, Rose BA, Stone MD, et al. A functional screen provides evidence for a conserved, regulatory, juxtamembrane phosphorylation site in guanylyl cyclase A and B. PLoS One 2012;7:e36747.
[31] Dickey DM, Burnett Jr JC, Potter LR. Novel bifunctional natriuretic peptides as potential therapeutics. J Biol Chem 2008;283:35003–9.
[32] Bryan PM, Potter LR. The atrial natriuretic peptide receptor (NPR-A/GC-A) is dephosphorylated by distinct microcystin-sensitive and magnesium-dependent protein phosphatases. J Biol Chem 2002;277:16041–7.
[33] Robinson JW, Potter LR. ATP potentiates competitive inhibition of guanylyl cyclase A and B by the staurosporine analog, Go6976: reciprocal regulation of ATP and GTP binding. J Biol Chem 2011;286:33841–4.
[34] Abbey-Hosch SE, Smirnov D, Potter LR. Differential regulation of NPR-B/GC-B by protein kinase C and calcium. Biochem Pharmacol 2005;70:686–94.

[35] Flora DR, Potter LR. Prolonged atrial natriuretic peptide exposure stimulates guanylyl cyclase-A degradation. Endocrinology 2010;151:2769–76.
[36] Fujishige K, Kotera J, Yanaka N, Akatsuka H, Omori K. Alteration of cGMP metabolism during chondrogenic differentiation of chondroprogenitor-like EC cells, ATDC5. Biochim Biophys Acta 1999;1452:219–27.
[37] Ivanova K, Heim JM, Gerzer R. Kinetic characterization of atrial natriuretic factor-sensitive particulate guanylate cyclase. Eur J Pharmacol 1990;189:317–26.
[38] Potter LR, Hunter T. Phosphorylation of the kinase homology domain is essential for activation of the A-type natriuretic peptide receptor. Mol Cell Biol 1998;18:2164–72.
[39] Chrisman TD, Garbers DL, Parks MA, Hardman JG. Characterization of particulate and soluble guanylate cyclases from rat lung. J Biol Chem 1975;250:374–81.
[40] Kimura H, Murad F. Evidence for two different forms of guanylate cyclase in rat heart. J Biol Chem 1974;249:6910–6.

Hindawi Publishing Corporation
BioMed Research International
Volume 2013, Article ID 428247, 8 pages
http://dx.doi.org/10.1155/2013/428247

Review Article

Regenerative Medicine for the Cornea

Yoshinori Oie and Kohji Nishida

Department of Ophthalmology, Osaka University Graduate School of Medicine, 2-2 Yamadaoka, Suita, Osaka 565-0871, Japan

Correspondence should be addressed to Yoshinori Oie; yoie@ophthal.med.osaka-u.ac.jp

Received 21 August 2013; Accepted 21 October 2013

Academic Editor: Ryuichi Morishita

Regenerative medicine for the cornea provides a novel treatment strategy for patients with corneal diseases instead of conventional keratoplasty. Limbal transplantation has been performed in patients with a limbal stem cell deficiency. This procedure requires long-term immunosuppression that involves high risks of serious eye and systemic complications, including infection, glaucoma, and liver dysfunction. To solve these problems, ocular surface reconstruction using cultured limbal or oral mucosal epithelial stem cells has been successfully applied to patients. However, cell sheets must be fabricated in a cell processing center (CPC) under good manufacturing practice conditions for clinical use, and the expenses of maintaining a CPC are too high for all hospitals to cover. Therefore, several hospitals should share one CPC to standardize and spread the application of regenerative therapy using tissue-engineered oral mucosal epithelial cell sheets. Consequently, we developed a cell transportation technique for clinical trial to bridge hospitals. This paper reviews the current status of regenerative medicine for the cornea.

1. The Structure of the Cornea

The cornea is an avascular and transparent tissue that forms part of the anterior ocular segment. Together with the sclera, it forms the outer shell of the eyeball. The cornea serves as the transparent window of the eye that allows light to enter, whereas the sclera provides a dark box that allows an image to form on the retina. The cornea is exposed to the outer environment, whereas the white sclera is covered with the semitransparent conjunctiva and is not directly exposed to the outside.

The central cornea is 515 μm thick [1]. It comprises an outer stratified squamous nonkeratinized epithelium, an inner connective tissue stroma, and the innermost layer, a cuboidal endothelium (Figure 1). Disorders in any of these layers can cause corneal opacity and visual disturbance: epithelial disorder (e.g., limbal stem cell deficiency), stromal disorder (e.g., corneal dystrophy), and endothelial disorder (e.g., bullous keratopathy).

2. Limbal Stem Cells

The corneal epithelium has five to seven cell layers and is 50–52 μm thick. It is composed of small basal cells, flattened middle cells (wing cells), and polygonal flattened superficial cells. Corneal epithelial stem cells (limbal stem cells) are thought to reside in the basal layer of the limbus, the transitional zone between the cornea and the conjunctiva (Figure 2) [2, 3]. Transient amplifying (TA) cells are generated by stem cells and then migrate into the central cornea. Although stem cells are low-cycling, TA cells proliferate rapidly.

Thoft and Friend hypothesized that corneal epithelial maintenance can be defined by the equation $X + Y = Z$, with X being the proliferation of basal epithelial cells; Y being the contribution to the cell mass by the centripetal movement of peripheral cells; and Z being the epithelial cell loss from the surface [4]. Therefore, the proliferation and migration of TA cells differentiated from stem cells play very important roles in the maintenance of corneal epithelium.

p63, ATP-binding cassette subfamily G member 2 (ABCG2), N-cadherin, K19, NGF receptors (TrkA), and integrin a6 have been reported as candidate markers of limbal stem cells. However, a specific marker has not yet been identified [4–9].

The palisades of Vogt are distinctive normal features of the human corneoscleral limbus [10] (Figure 3). They are more discrete in younger and more heavily pigmented

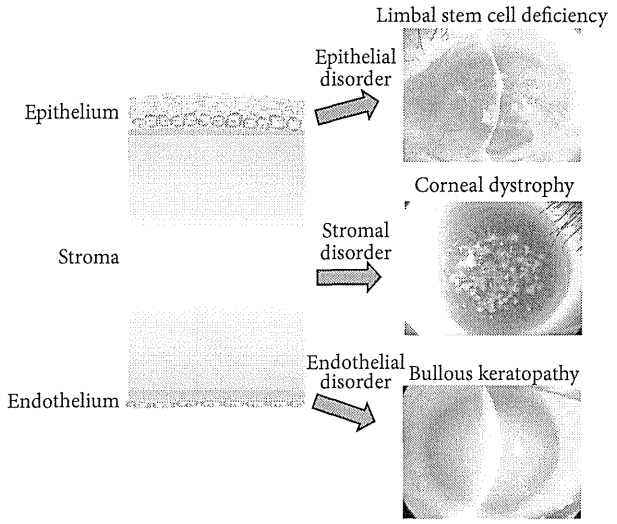

FIGURE 1: The structure and disorders of the cornea. The cornea consists of three layers: epithelium, stroma, and endothelium. Visual acuity can be affected by disorders of any of these layers, including limbal stem cell deficiency, corneal dystrophy, and bullous keratopathy.

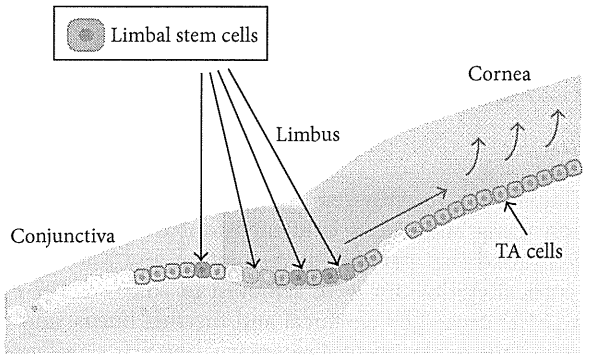

FIGURE 2: Limbal stem cells. Limbal stem cells are believed to be located within the basal layer of the limbus. Transient amplifying (TA) cells are progenitor cells that differentiate from limbal stem cells and then migrate into the central cornea.

individuals, and they appear more regular and prominent at the lower limbus than at the upper limbus. They are observed infrequently along the horizontal meridian.

Lately, a new phenomenon, "limbal epithelial crypts (LEC)," has been reported as a putative limbal stem cell niche [11, 12]. Cells within LEC have the phenotype of CK3−/CK19+/CD34−/Vimentin+/p63+/Connexin43+/MIB (Ki67)−.

3. Limbal Stem Cell Deficiency

If limbal stem cells are completely absent, vascularized conjunctival epithelium invades into the cornea. The condition is called limbal stem cell deficiency (LSCD) (Figure 4). It results in a corneal neovascularization and opacification that disturbs visual acuity. The causative diseases can be classified

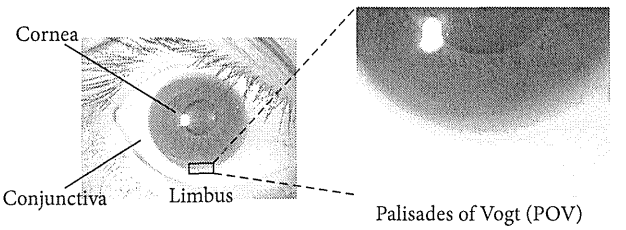

FIGURE 3: Palisades of Vogt (POV). A slit lamp examination reveals the limbus-specific feature, the "palisades of Vogt" (POV).

into four groups: (1) congenital diseases caused by congenital aplasia of stem cells (e.g., aniridia, sclerocornea); (2) diseases with an external cause, involving the loss of stem cells due to trauma (e.g., thermal, alkali, and acid burns); (3) diseases involving internal, stem cell exhaustion, such as Stevens-Johnson syndrome and ocular cicatricial pemphigoid; and (4) idiopathic diseases of unknown cause [13].

4. Limbal Transplantation

In patients with unilateral limbal stem cell deficiency, autologous limbal transplantation can be used to achieve surface reconstruction of the cornea [14]. However, this procedure requires a large limbal graft from the healthy eye (incurring a risk of causing limbal stem cell deficiency in the healthy eye [15]) and is not applicable to bilaterally affected patients [16]. Limbal-allograft transplantation can be performed in patients with unilateral or bilateral deficiencies [17, 18]. However, it has two main problems: postoperative complications and a donor shortage.

Postoperative complications include rejection and bacterial or fungal keratitis [19–22]. Limbal transplantation requires long-term immunosuppression, which involves high risks of serious eye and systemic complications, including infection and liver and kidney dysfunction. Even with immunosuppression, graft failure is common in patients with Stevens-Johnson syndrome or ocular pemphigoid due to serious preoperative conditions, such as persistent inflammation of the ocular surface, abnormal epithelial differentiation of the ocular surface, severe dry eye, and lid-related abnormalities.

Donor shortage is also a major problem in many countries, including Japan. The Japan Eye Bank Association reported that the number of patients waiting for keratoplasty was 2,286 but that the number of donors was 891 in Japan in 2012.

5. Regenerative Medicine and Tissue Engineering

Langer and Vacanti established the field of "tissue engineering" [23, 24]. Tissue engineering is an interdisciplinary field that applies the principles of engineering and the life sciences toward the development of biological substitutes that restore, maintain, or improve tissue function. This technology has been applied to various tissues and organs, including the

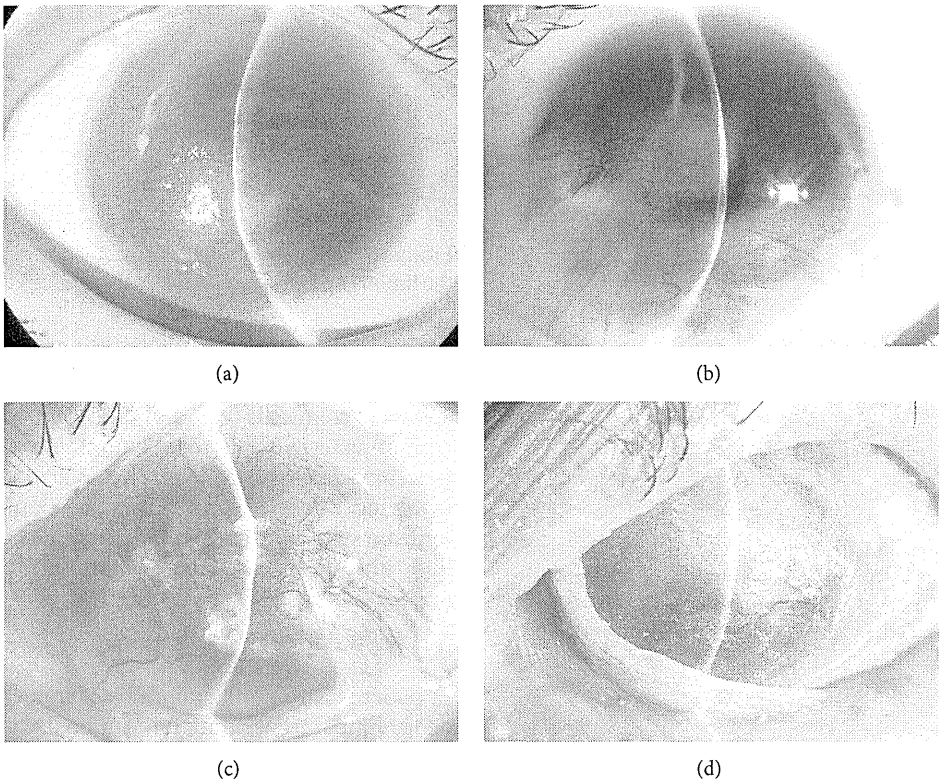

FIGURE 4: Slit lamp photographs of patients with a limbal stem cell deficiency. (a) Aniridia; (b) alkali burn; (c) ocular cicatricial pemphigoid; (d): Stevens-Johnson syndrome.

skin, cornea, cartilage, and heart [25–34]. Enormous promise has been ascribed to this technology because it offers a paradigm shift from conventional organ transplantation to a novel treatment strategy that relies on cultured stem cells. Furthermore, this technique could potentially solve the two main problems of corneal transplantation.

6. Cultivated Limbal Epithelial Cell Transplantation (CLET)

Autologous cultivated limbal epithelial cell transplantation was initially reported by Pellegrini and colleagues [26]. They reported that two patients with LSCD caused by alkali burns were restored using autologous cultivated corneal epithelium, and the outcome persisted for more than two years after grafting. This report is the first of a clinical application in the field of regenerative medicine for the cornea.

Following this report, many investigators have reported the effectiveness and safety of CLET [35–39]. The amniotic membrane and fibrin glue have been mainly used as substrates for cultivated cells. The amniotic membrane has been used as a natural substrate because it can expand into the stem cell niche [40]. Various cytokines released from the amniotic membrane, such as epidermal growth factor, keratinocyte growth factor, hepatocyte growth factor, nerve growth factor, and basic fibroblast growth factor, have been reported to play important roles within the niche of limbal stem cells. The amniotic basement membrane offers a basement membrane for corneal epithelial cell adhesion.

Rama et al. recently reported long-term corneal regeneration using autologous cultivated limbal stem cells [29]. They showed that permanent restoration and a renewal of the corneal epithelium were achieved in 76.6% of 107 eyes with LSCD caused by chemical and thermal burns, and the success of the ocular surface reconstruction was significantly associated with the percentage of p63-bright, holoclone-forming stem cells in culture. No severe adverse events were observed. Their results demonstrated the effectiveness and safety of CLET and the importance of the stem cell population within the cultured cells.

7. Cultivated Oral Mucosal Epithelial Cell Transplantation (COMET)

Although CLET can be applied to patients with unilateral LSCD, it cannot be applied to patients with bilateral disease because they have completely lost their own limbal stem cells as a cell source. Consequently, autologous cultivated oral mucosal epithelial cell transplantation (COMET) has been developed for patients with bilateral LSCD [28, 41]. Even in unilateral cases, some patients wish to avoid tampering with the limbus of their unaffected eye.

We use a temperature-responsive culture dish to fabricate oral mucosal cells [42]. Cell sheets are cultivated on the dishes coated with a temperature-responsive polymer, poly(N-isopropylacrylamide) (PIPAAm), which is hydrophobic below 32°C and hydrophilic above 32°C (Figure 5).

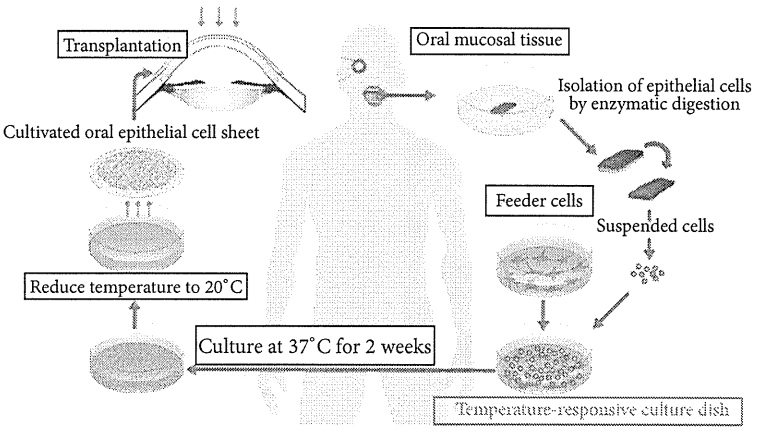

FIGURE 5: Ocular surface reconstruction via the autologous transplantation of tissue-engineered cell sheets fabricated from oral mucosal epithelial cells. Oral mucosal tissue containing whole epithelial cell layers was excised from the oral cavities of the patient. The cells were then seeded onto a temperature-responsive culture dish. The cultured cells were harvested as a cell sheet by reducing the culture temperature. The cells were then transplanted onto the corneal surfaces of the patient.

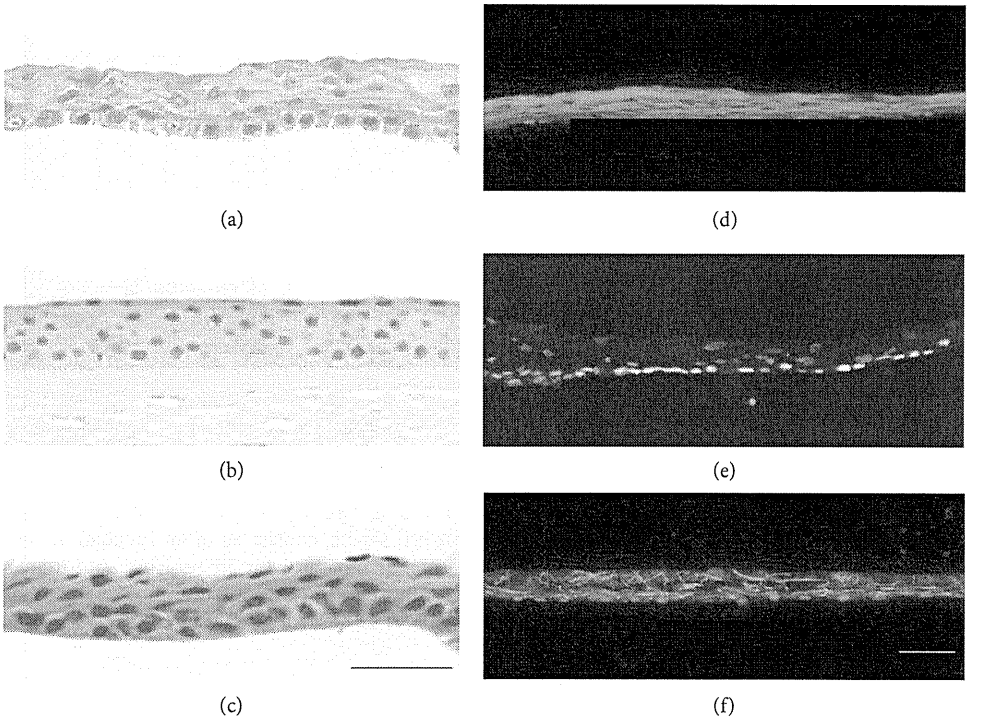

FIGURE 6: Histological and immunohistochemical analyses of cell sheets. HE staining was performed for an oral mucosal epithelial cell sheet (a), a normal cornea (b), and a corneal epithelial cell sheet (c). Human oral mucosal epithelial cell sheets were stained with antikeratin 3/76 (d), anti-p63 (e), and anti-ZO-1 (f) antibodies. Nuclei were costained with Hoechst 33342. Scale bars: 50 μm.

This change releases the cell sheet, allowing it to be removed without destroying the cell-cell or the cell-extracellular matrix interactions within the cell sheet. Therefore, cultivated oral mucosal epithelial cells can be harvested using a temperature reduction without the use of enzymes.

The cell morphology of an oral mucosal epithelial cell sheet fabricated on a temperature-responsive culture dish is similar to that of the normal cornea or a corneal epithelial cell sheet (Figure 6). It consists of approximately four epithelial layers, flattened superficial cells, and small basal cells with a high C/D ratio. Keratin 3/76, a marker of corneal and oral mucosal epithelium, is positive in the oral mucosal epithelial cell sheet. p63, a putative stem cell marker, is positive for basal cells. ZO-1, a marker of tight junctions, is positive, particularly between superficial cells. The oral mucosal epithelial cell sheet is assumed to have a similar phenotype to that of corneal epithelium as well as enough stem cells and a barrier capability for ocular surface reconstruction. We have already

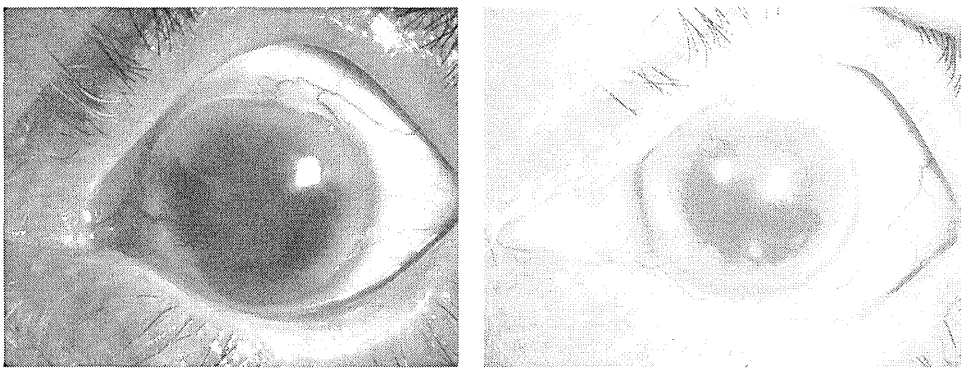

(a) (b)

FIGURE 7: Slit lamp photographs of patients before and after cultivated oral mucosal epithelial cell transplantation. (a) The right eye has a total limbal stem cell deficiency caused by ocular cicatricial pemphigoid. The VA is 20/2000. (b) Eight years postoperatively, the corneal epithelial clarity was well maintained. The VA is 20/222 despite macular degeneration.

begun a clinical study using this technique and achieved favorable results (Figure 7) [28].

There has been no report on severe adverse events including development of malignant tumor following COMET. However, if there is a problem, we can easily observe and remove transplanted oral mucosal cells from ocular surface. From that point of view, ocular surface would be the ideal environment for application of this kind of new treatment.

Longstanding survival of transplanted oral mucosal epithelial cells remains unclear. Because autologous oral mucosal cells are used as a cell source, there is no method to distinguish transplanted cells and native cells from host tissue. Even if phenotype of transplanted oral mucosal epithelial cells is maintained, there remains the possibility that host conjunctival cells invaded into cornea and changed the phenotype. However, analyses on phenotype of corneal epithelium excised during keratoplasty following COMET suggest longstanding survival of transplanted oral mucosal epithelial cells. Nakamura et al. reported that phenotype of transplanted cultivated oral epithelial cells (keratin 3[+], Muc5ac[−]) was maintained in clinically successful COMET grafts, and the phenotype was not maintained in failed grafts [43]. Chen et al. showed that all specimens were unanimously positive for K3, -4, and -13 but negative for K8 and MUC5AC, suggesting that the keratinocytes were oral-mucosa-derived [44].

Ohki et al. also applied tissue-engineered oral mucosal epithelial cell sheets to prevent esophageal stricture after endoscopic submucosal dissection [45]. Oral mucosal epithelial cells can be applied for other diseases in the future.

8. Transportation Technique for Regenerative Medicine

The cell sheets must be fabricated in a cell processing center (CPC) under good manufacturing practice (GMP) conditions for clinical use. However, the expenses for a CPC are extremely high, and it is impossible for all hospitals to cover the cost. Therefore, multiple hospitals should share

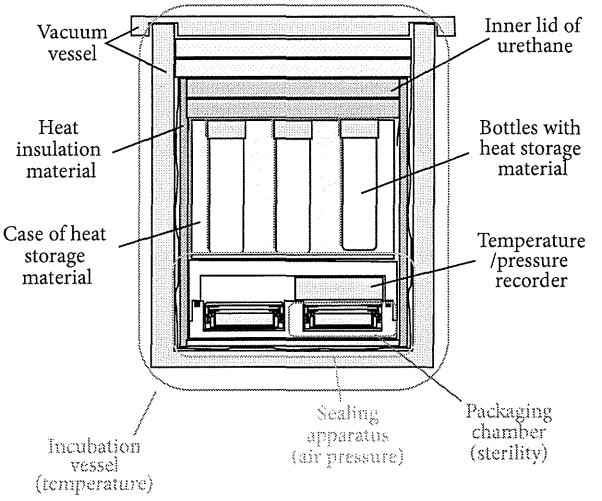

FIGURE 8: Cross-sectional view of a cell transportation container for cell sheets, consisting of an incubation vessel for temperature, a sealing apparatus for air pressure, and four packaging chambers for sterility. Bottles with heat storage material are set inside the incubation vessel.

one CPC to standardize and spread regenerative therapy using tissue-engineered oral mucosal epithelial cell sheets. Therefore, the development of cell transportation techniques is necessary for bridging many hospitals.

We developed a transportation container with three basic functions: maintaining a constant interior temperature, air pressure, and sterility (Figure 8) [46]. The interior temperature and air pressure were monitored by a sensor. Human oral mucosal epithelial cells obtained from two healthy volunteers were cultured on temperature-responsive culture dishes. The epithelial cell sheets were transported via airplane between Osaka University and Tohoku University using the developed cell transportation container. Histological and immunohistochemical analyses and flow cytometric analyses for cell viability and cell purity were performed on the cell sheets before and 12 h after transportation to determine the

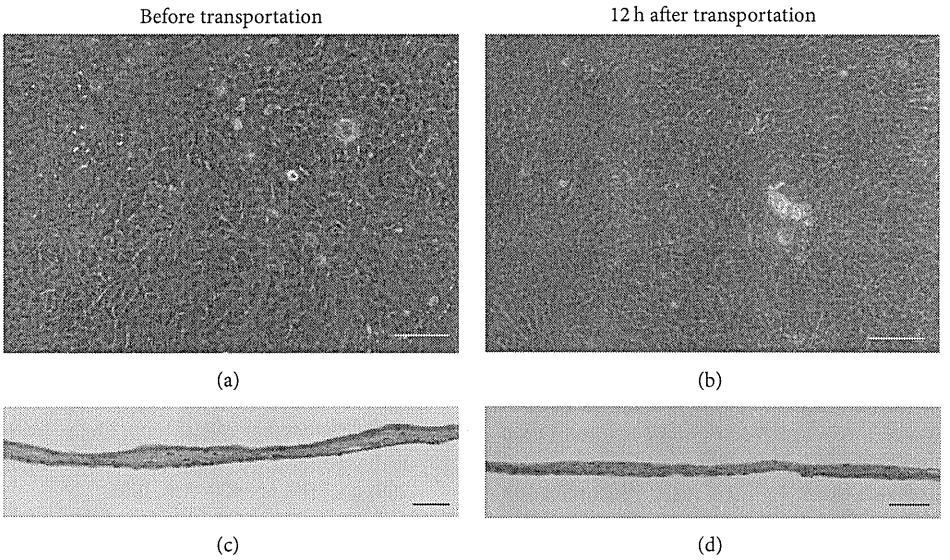

FIGURE 9: Human oral mucosal epithelial cell sheets before and 12 h after transportation. The cell morphology was examined using phase-contrast microscopy (a, b) and HE staining (c, d). Scale bars: 100 μm (a, b), 50 μm (c, d).

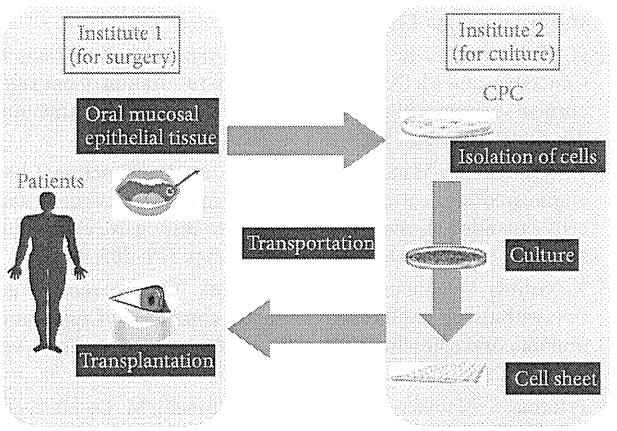

FIGURE 10: Multicenter clinical study of a cell sheet transportation system. Oral surgery for mucosal tissue and cell sheet transplantation are performed at institute 1; the cell sheets are cultured in the CPC at institute 2.

effect of transportation on the cell sheets. Sterility tests and screening for endotoxins and mycoplasma in the cell sheets were performed before and after transportation.

During transportation via airplane, the temperature inside the container was maintained above 32°C, and the air pressure did not fluctuate more than 10 hPa. The cell sheets were well stratified and successfully harvested before and after transportation (Figure 9). The expression patterns of keratin 3/76, p63, ZO-1, and MUC16 remained consistent before and after transportation. The cell viability was 72.0% before transportation and 77.3% after transportation. The epithelial purity was 94.6% before transportation and 87.9% after transportation. Sterility tests and screening for endotoxins and mycoplasma were negative for all cell sheets.

We are conducting a multicenter clinical study using the transportation technique described herein (Figure 10). In this clinical study, we will harvest oral mucosal epithelial tissues from patients at institute 1 and transport them to institute 2. At institute 2, a cell sheet will be fabricated at the CPC. Next, the cell sheet will be sent to institute 1 for transplantation. We will culture oral mucosal epithelial cells from two other institutes in Osaka University. Culturing at a single CPC enables better control of the quality of the tissue-engineered human oral mucosal epithelial cell sheet. If this effort is successful, we will be able to treat many patients in many hospitals all over the world without the need for a CPC.

The newly developed transportation technique for air travel is an essential technology for regenerative medicine and promotes the standardization and spread of regenerative therapies.

9. Conclusion

Many researchers have engaged in basic and clinical study in the fields of stem cell and regenerative medicine for the cornea. However, there are no government-approved tissue-engineered medical products for the cornea so far. Although first-in human clinical study using a novel cell source or technology is both sensational and impressive, efforts to turn this established technique into a standardized therapy should be a continuous process. We are struggling to make oral mucosal epithelial cell sheets an approved medical device. We believe that, once approved, this medical product will help visually impaired patients all over the world and that this goal can be achieved in the near future.

References

[1] C. J. Rapuano, J. A. Fishbaugh, and D. J. Strike, "Nine point corneal thickness measurements and keratometry readings in

normal corneas using ultrasound pachymetry," *Insight*, vol. 18, no. 4, pp. 16–22, 1993.

[2] A. Schermer, S. Galvin, and T. T. Sun, "Differentiation-related expression of a major 64K corneal keratin in vivo and in culture suggests limbal location of corneal epithelial stem cells," *Journal of Cell Biology*, vol. 103, no. 1, pp. 49–62, 1986.

[3] G. Cotsarelis, S. Z. Cheng, G. Dong, T. T. Sun, and R. M. Lavker, "Existence of slow-cycling limbal epithelial basal cells that can be preferentially stimulated to proliferate: implications on epithelial stem cells," *Cell*, vol. 57, no. 2, pp. 201–209, 1989.

[4] G. Pellegrini, P. Rama, F. Mavilio, and M. De Luca, "Epithelial stem cells in corneal regeneration and epidermal gene therapy," *Journal of Pathology*, vol. 217, no. 2, pp. 217–228, 2009.

[5] R. A. Thoft and J. Friend, "The X, Y, Z hypothesis of corneal epithelial maintenance," *Investigative Ophthalmology and Visual Science*, vol. 24, no. 10, pp. 1442–1443, 1983.

[6] U. Schlötzer-Schrehardt and F. E. Kruse, "Identification and characterization of limbal stem cells," *Experimental Eye Research*, vol. 81, no. 3, pp. 247–264, 2005.

[7] R. Hayashi, M. Yamato, H. Sugiyama et al., "N-cadherin is expressed by putative stem/progenitor cells and melanocytes in the human limbal epithelial stem cell niche," *Stem Cells*, vol. 25, no. 2, pp. 289–296, 2007.

[8] R. Hayashi, M. Yamato, T. Saito et al., "Enrichment of corneal epithelial stem/progenitor cells using cell surface markers, integrin α6 and CD71," *Biochemical and Biophysical Research Communications*, vol. 367, no. 2, pp. 256–263, 2008.

[9] K. Watanabe, K. Nishida, M. Yamato et al., "Human limbal epithelium contains side population cells expressing the ATP-binding cassette transporter ABCG2," *FEBS Letters*, vol. 565, no. 1-3, pp. 6–10, 2004.

[10] H. S. Dua, V. A. Shanmuganathan, A. O. Powell-Richards, P. J. Tighe, and A. Joseph, "Limbal epithelial crypts: a novel anatomical structure and a putative limbal stem cell niche," *British Journal of Ophthalmology*, vol. 89, no. 5, pp. 529–532, 2005.

[11] V. A. Shanmuganathan, T. Foster, B. B. Kulkarni et al., "Morphological characteristics of the limbal epithelial crypt," *British Journal of Ophthalmology*, vol. 91, no. 4, pp. 514–519, 2007.

[12] M. F. Goldberg and A. J. Bron, "Limbal palisades of Vogt," *Transactions of the American Ophthalmological Society*, vol. 80, pp. 155–171, 1982.

[13] K. Nishida, "Tissue engineering of the cornea," *Cornea*, vol. 22, no. 7, pp. S28–S34, 2003.

[14] K. R. Kenyon and S. C. G. Tseng, "Limbal autograft transplantation for ocular surface disorders," *Ophthalmology*, vol. 96, no. 5, pp. 709–723, 1989.

[15] J. J. Y. Chen and S. C. G. Tseng, "Corneal epithelial wound healing in partial limbal deficiency," *Investigative Ophthalmology and Visual Science*, vol. 31, no. 7, pp. 1301–1314, 1990.

[16] H. S. Dua and A. Azuara-Blanco, "Autologous limbal transplantation in patients with unilateral corneal stem cell deficiency," *British Journal of Ophthalmology*, vol. 84, no. 3, pp. 273–278, 2000.

[17] K. Tsubota, Y. Satake, M. Kaido et al., "Treatment of severe ocular-surface disorders with corneal epithelial stem-cell transplantation," *New England Journal of Medicine*, vol. 340, no. 22, pp. 1697–1703, 1999.

[18] D. T. H. Tan, J. K. G. Dart, E. J. Holland, and S. Kinoshita, "Corneal transplantation," *The Lancet*, vol. 379, no. 9827, pp. 1749–1761, 2012.

[19] C. M. Samson, C. Nduaguba, S. Baltatzis, and C. S. Foster, "Limbal stem cell transplantation in chronic inflammatory eye disease," *Ophthalmology*, vol. 109, no. 5, pp. 862–868, 2002.

[20] L. Ilari and S. M. Daya, "Long-term outcomes of keratolimbal allograft for the treatment of severe ocular surface disorders," *Ophthalmology*, vol. 109, no. 7, pp. 1278–1284, 2002.

[21] J. Shimazaki, S. Shimmura, H. Fujishima, and K. Tsubota, "Association of preoperative tear function with surgical outcome in severe Stevens-Johnson syndrome," *Ophthalmology*, vol. 107, no. 8, pp. 1518–1523, 2000.

[22] J. A. Gomes, M. S. Santos, A. S. Ventura, W. B. Donato, M. C. Cunha, and A. L. Höfling-Lima, "Amniotic membrane with living related corneal limbal/conjunctival allograft for ocular surface reconstruction in Stevens-Johnson syndrome," *Archives of Ophthalmology*, vol. 121, no. 10, pp. 1369–1374, 2003.

[23] R. Langer and J. P. Vacanti, "Tissue engineering," *Science*, vol. 260, no. 5110, pp. 920–926, 1993.

[24] J. P. Vacanti and R. Langer, "Tissue engineering: the design and fabrication of living replacement devices for surgical reconstruction and transplantation," *The Lancet*, vol. 354, no. 1, pp. S32–S34, 1999.

[25] G. G. Gallico III, N. E. O'Connor, and C. C. Compton, "Permanent coverage of large burn wounds with autologous cultured human epithelium," *New England Journal of Medicine*, vol. 311, no. 7, pp. 448–451, 1984.

[26] G. Pellegrini, C. E. Traverso, A. T. Franzi, M. Zingirian, R. Cancedda, and M. De Luca, "Long-term restoration of damaged corneal surfaces with autologous cultivated corneal epithelium," *The Lancet*, vol. 349, no. 9057, pp. 990–993, 1997.

[27] K. Nishida, M. Yamato, Y. Hayashida et al., "Functional bioengineered corneal epithellial sheet grafts from corneal stem cells expanded ex vivo on a temperature-responsive cell culture surface," *Transplantation*, vol. 77, no. 3, pp. 379–385, 2004.

[28] K. Nishida, M. Yamato, Y. Hayashida et al., "Corneal reconstruction with tissue-engineered cell sheets composed of autologous oral mucosal epithelium," *New England Journal of Medicine*, vol. 351, no. 12, pp. 1187–1196, 2004.

[29] P. Rama, S. Matuska, G. Paganoni, A. Spinelli, M. De Luca, and G. Pellegrini, "Limbal stem-cell therapy and long-term corneal regeneration," *New England Journal of Medicine*, vol. 363, no. 2, pp. 147–155, 2010.

[30] M. Brittberg, A. Lindahl, A. Nilsson, C. Ohlsson, O. Isaksson, and L. Peterson, "Treatment of deep cartilage defects in the knee with autologous chondrocyte transplantation," *New England Journal of Medicine*, vol. 331, no. 14, pp. 889–895, 1994.

[31] M. Ochi, Y. Uchio, K. Kawasaki, S. Wakitani, and J. Iwasa, "Transplantation of cartilage-like tissue made by tissue engineering in the treatment of cartilage defects of the knee," *Journal of Bone and Joint Surgery B*, vol. 84, no. 4, pp. 571–578, 2002.

[32] P. Menasché, O. Alfieri, S. Janssens et al., "The myoblast autologous grafting in ischemic cardiomyopathy (MAGIC) trial: first randomized placebo-controlled study of myoblast transplantation," *Circulation*, vol. 117, no. 9, pp. 1189–1200, 2008.

[33] S. Miyagawa, G. Matsumiya, T. Funatsu et al., "Combined autologous cellular cardiomyoplasty using skeletal myoblasts and bone marrow cells for human ischemic cardiomyopathy with left ventricular assist system implantation: report of a case," *Surgery Today*, vol. 39, no. 2, pp. 133–136, 2009.

[34] Y. Sawa and S. Miyagawa, "Cell sheet technology for heart failure," *Current Pharmaceutical Biotechnology*, vol. 14, no. 1, pp. 61–66, 2013.

[35] R. J. F. Tsai, L. M. Li, and J. K. Chen, "Reconstruction of damaged corneas by transplantation of autologous limbal epithelial cells," *New England Journal of Medicine*, vol. 343, no. 2, pp. 86–93, 2000.

[36] P. Rama, S. Bonini, A. Lambiase et al., "Autologous fibrin-cultured limbal stem cells permanently restore the corneal surface of patients with total limbal stem cell deficiency," *Transplantation*, vol. 72, no. 9, pp. 1478–1485, 2001.

[37] N. Koizumi, T. Inatomi, T. Suzuki, C. Sotozono, and S. Kinoshita, "Cultivated corneal epithelial stem cell transplantation in ocular surface disorders," *Ophthalmology*, vol. 108, no. 9, pp. 1569–1574, 2001.

[38] V. S. Sangwan, G. K. Vemuganti, G. Iftekhar, A. K. Bansal, and G. N. Rao, "Use of autologous cultured limbal and conjunctival epithelium in a patient with severe bilateral ocular surface disease induced by acid injury: a case report of unique application," *Cornea*, vol. 22, no. 5, pp. 478–481, 2003.

[39] I. R. Schwab, M. Reyes, and R. R. Isseroff, "Successful transplantation of bioengineered tissue replacements in patients with ocular surface disease," *Cornea*, vol. 19, no. 4, pp. 421–426, 2000.

[40] M. Grueterich, E. M. Espana, and S. C. G. Tseng, "Ex vivo expansion of limbal epithelial stem cells: amniotic membrane serving as a stem cell niche," *Survey of Ophthalmology*, vol. 48, no. 6, pp. 631–646, 2003.

[41] T. Nakamura, T. Inatomi, C. Sotozono, T. Amemiya, N. Kanamura, and S. Kinoshita, "Transplantation of cultivated autologous oral mucosal epithelial cells in patients with severe ocular surface disorders," *British Journal of Ophthalmology*, vol. 88, no. 10, pp. 1280–1284, 2004.

[42] T. Okano, N. Yamada, H. Sakai, and Y. Sakurai, "A novel recovery system for cultured cells using plasma-treated polystyrene dishes grafted with poly(N-isopropylacrylamide)," *Journal of Biomedical Materials Research*, vol. 27, no. 10, pp. 1243–1251, 1993.

[43] T. Nakamura, T. Inatomi, L. J. Cooper, H. Rigby, N. J. Fullwood, and S. Kinoshita, "Phenotypic investigation of human eyes with transplanted autologous cultivated oral mucosal epithelial sheets for severe ocular surface diseases," *Ophthalmology*, vol. 114, no. 6, pp. 1080–1088, 2007.

[44] H. C. Chen, H. L. Chen, C. C. Chen et al., "Persistence of transplanted oral mucosal epithelial cells in human cornea," *Investigative Ophthalmology & Visual Science*, vol. 50, no. 10, pp. 4660–4668, 2009.

[45] T. Ohki, M. Yamato, M. Ota et al., "Prevention of esophageal stricture after endoscopic submucosal dissection using tissue-engineered cell sheets," *Gastroenterology*, vol. 143, no. 3, pp. 582–588, 2012.

[46] Y. Oie, T. Nozaki, H. Takayanagi et al., "Development of a cell sheet transportation technique for regenerative medicine," *Tissue Engineering C*, 2013.

Biochemical and Biophysical Research Communications 432 (2013) 509–512

Contents lists available at SciVerse ScienceDirect

Biochemical and Biophysical Research Communications

journal homepage: www.elsevier.com/locate/ybbrc

Molecular genetic analysis of primary open-angle glaucoma, normal tension glaucoma, and developmental glaucoma for the *VAV2* and *VAV3* gene variants in Japanese subjects

Dong Shi [a,b,*], Yoshimasa Takano [b], Toru Nakazawa [b], MinGe Mengkegale [b], Shunji Yokokura [b], Kohji Nishida [b,c], Nobuo Fuse [b,d]

[a] Department of Ophthalmology, The Fourth Affiliated Hospital, China Medical University, 11 Xinhua Road, Heping District, Shenyang, Liaoning 110005, China
[b] Department of Ophthalmology, Tohoku University Graduate School of Medicine, 1-1 Seiryo-machi, Aoba-ku, Sendai, Miyagi 980-8574, Japan
[c] Department of Ophthalmology, Osaka University Graduate School of Medicine, Suita, Osaka 565-0871, Japan
[d] Department of Integrative Genomics, Tohoku Medical Megabank Organization, 1-1 Seiryo-machi, Aoba-ku, Sendai, Miyagi 980-8574, Japan

ARTICLE INFO

Article history:
Received 26 January 2013
Available online 10 February 2013

Keywords:
POAG
NTG
DG
VAV2
VAV3
Gene screening

ABSTRACT

The *VAV2* and *VAV3* genes have been implicated as being causative for primary open angle glaucoma (POAG) in the Japanese. We studied 168 unrelated Japanese patients with primary open-angle glaucoma (POAG), 163 unrelated Japanese patients with normal tension glaucoma (NTG), 45 unrelated Japanese patients with developmental glaucoma (DG), and 180 ethnically matched normal controls, to determine whether variants in the vav 2 guanine nucleotide exchange factor (*VAV2*) and vav 3 guanine nucleotide exchange factor (*VAV3*) genes are associated with POAG, NTG, or DG in the Japanese. Genomic DNA was extracted from peripheral blood leukocytes, and variants in the *VAV2* and *VAV3* genes were amplified by polymerase chain reaction (PCR) and directly sequenced. Two variants were identified: rs2156323 in *VAV2* and rs2801219 in *VAV3*. The variants and the prevalence of POAG, NTG, and DG in unrelated Japanese patients indicated that the variants were not involved in the pathogenesis of POAG, NTG, or DG.

1. Introduction

Glaucoma is a complex, heterogeneous disease characterized by a progressive degeneration of the optic nerve axons, and it is the second highest cause of blindness, affecting approximately 70 million people worldwide [1]. Because the optic nerve axons degenerate in eyes with glaucoma, visual field defects develop. Primary open-angle glaucoma (POAG), the most common type of glaucoma, is associated with elevated intraocular pressure (IOP). Patients with POAG who have IOP in the normal range (<22 mmHg) are classified as having normal tension glaucoma (NTG) [2]. The prevalence of NTG is significantly higher among the Japanese than among Caucasians [3,4].

Although the precise molecular basis of POAG has not been established, it is most likely a genetically heterogeneous disorder caused by the interaction of multiple genes and environmental factors [5,6]. Several genetic loci that contribute to susceptibility to POAG have been identified. To date, at least 15 loci (GLC1A to GLC1O) have been linked to POAG, and three genes have been identified: the myocilin (*MYOC*) gene [7], the optineurin (*OPTN*) gene [8], and the WD-repeat domain 36 (*WDR36*) gene [9]. The *MYOC* gene encodes for myocilin and is mutated in juvenile-onset primary open-angle glaucoma. The optineurin (*OPTN*) gene is mutated in families with autosomal dominant, adult-onset POAG, including some with normal tension glaucoma. The *WDR36* gene is a relatively new causative gene for adult-onset POAG. However, several studies have reported that the *OPTN* and *WDR36* variants do not predispose subjects to POAG/NTG [10–15].

Recently, the genes for vav 2 guanine nucleotide exchange factor (*VAV2*) (OMIM 600428) and vav 3 guanine nucleotide exchange factor (*VAV3*) (OMIM 605541) were reported to cause POAG in the Japanese [10]. The authors provided functional evidence suggesting that *Vav2*- and *Vav2/Vav3*- deficient mice had a spontaneous glaucoma phenotype resulting in progressive iridocorneal changes and elevated IOPs. In addition, a genome-wide association study (GWAS) that screened for glaucoma susceptibility loci using single nucleotide polymorphism (SNP) analysis identified intronic SNPs in *VAV2* (rs2156323) and *VAV3* (rs2801219) as candidates for genes associated with POAG in Japanese glaucoma patients.

An accurate diagnostic test for pre-symptomatic individuals at risk for glaucoma is needed, and screening for the *VAV2* and *VAV3* genes may identify pre-symptomatic cases in the general population. Thus, the purpose of this study was to determine

* Corresponding author at: Department of Ophthalmology, The Fourth Affiliated Hospital, China Medical University, 11 Xinhua Road, Heping District, Shenyang, Liaoning 110005, China. Fax: +86 24 62689311.
E-mail addresses: locust.stone@hotmail.com, shidong@mail.cmu.edu.cn (D. Shi).

0006-291X/$ - see front matter © 2013 Elsevier Inc. All rights reserved.
http://dx.doi.org/10.1016/j.bbrc.2013.02.003

whether variants in the *VAV2* and *VAV3* genes contribute to POAG, NTG, and developmental glaucoma (DG) in Japanese patients.

2. Patients and methods

2.1. Patients

One hundred and sixty eight unrelated Japanese patients with POAG (89 men and 79 women; mean age 63.6 ± 14.4 years), 163 unrelated Japanese patients with NTG (86 men and 77 women; mean age 61.8 ± 13.7 years), and 45 unrelated Japanese patients with DG (18 men and 27 women; mean age 30.7 ± 10.7 years), who were diagnosed in the ophthalmology clinic at the Tohoku University Hospital, Sendai, Japan, were studied. The percentages of patients from each of the different regions of Japan were as follows: 70% of the patients were from the northern region, 20% were from the eastern region, and <10% were from the western region of Japan.

The purpose and procedures of the experiment were explained to all the patients, and their informed consent was obtained. The procedures used conformed to the tenets of the Declaration of Helsinki, and the Tohoku University Institutional Review Board approved this study.

Routine ophthalmic examinations were performed on all the patients. The criteria for classifying a patient as having POAG were the following: (1) applanation IOP >22 mmHg in each eye; (2) glaucomatous cupping in each eye, including a cup-to-disc ratio >0.7; (3) visual field defects, determined by Goldmann and/or Humphrey perimetry, that are consistent with glaucomatous cupping in at least one eye; and (4) an open anterior chamber angle. The criteria for NTG were the following: (1) applanation IOP less than 22 mmHg in both eyes at each examination; and (2) the same characteristics as the POAG group. Patients with glaucoma due to secondary causes, e.g., trauma, uveitis, or steroid use, were excluded.

Control subjects (95 men and 85 women; mean age 68.0 ± 7.7 years) were characterized by the following characteristics: (1) IOP <22 mmHg; (2) normal optic discs; and (3) no family history of glaucoma. To decrease the chance of including individuals with pre-symptomatic glaucoma in this group, we studied individuals who were older than 60.

2.2. Sample preparation and variant screening

Genomic DNA was extracted from peripheral blood leukocytes and purified using the Qiagen QIAamp Blood Kit (Qiagen, USA). The SNPs rs2156323 (*VAV2*) and rs2801219 (*VAV3*) and their flanking regions were amplified by polymerase chain reaction (PCR) using 0.5 μM intronic primers in an amplification mixture (25 μl) containing 0.2 mM dNTPs and 0.5 U Ex Taq polymerase (Takara), with the addition of 30 ng of template DNA at an annealing temperature of 60° C. The oligonucleotides for amplification and sequencing were selected using Primer3 software (http://frodo.wi.mit.edu/cgi-bin/primer3/primer3_www.cgi/, Massachusetts Institute of Technology, Cambridge, MA).

The PCR fragments were purified with ExoSAP-IT (USB, Cleveland, Ohio, USA) and were sequenced with the BigDye™ Terminator Cycle Sequencing Ready Reaction Kit (Perkin-Elmer, Foster City, California, USA) on an automated DNA sequencer (ABI PRISM™ 3100 Genetic Analyzer, Perkin-Elmer).

2.3. Statistical analyses

Differences in the genotype frequencies among the cases and controls were tested using Fisher's exact test, depending on the cell counts. Odds ratios (approximating relative risk) were calculated to measure the association between the WDR36 genotype and the POAG/NTG phenotype, and the effects of the mutant allele were assumed to be dominant (wild/wild vs. wild/mutant and mutant/mutant combined). For each odds ratio, a *P* value and the 95% confidence intervals were calculated. The inferred haplotypes and LD, expressed as D' [11] and quantified between all pairs of biallelic loci, were estimated using the SNPAlyze program version 4.0 (Dynacom, Yokohama, Japan). The significance of the associations was determined by contingency table analysis using the chi-square test or Fisher's exact test. The Hardy–Weinberg equilibrium was analyzed using the gene frequencies obtained by simple gene counting and the chi-square test with Yates' correction for comparing observed and expected values. For general stand-alone statistical power analysis, we used G*Power [12]. G*Power computes the power values for given sample sizes, effect sizes, and alpha levels (post hoc power analyses), and the sample sizes for given effect sizes, alpha levels, and power values (a priori power analyses).

3. Results

3.1. Allelic frequencies for rs2156323 SNP in VAV2 and rs2801219 SNP in VAV3

Two variants were identified: rs2156323 in *VAV2* and rs2801219 in *VAV3*. The allelic frequencies for rs2156323 in *VAV2* and rs2801219 in *VAV3* for POAG, NTG, DG, and the control subjects are presented in Table 1. The allele frequencies of rs2156323 in *VAV2* in the POAG, the NTG, and the DG groups were not significantly different from the control group (minor allele frequency 0.051, 0.049, 0.022 vs. 0.036, respectively; $P = 0.35$, 0.40, and 0.51, respectively). The allele frequency of rs2801219 in *VAV3* was also not significantly higher in the two groups than in the control group (minor allele frequency 0.211, 0.236, 0.244 vs. 0.197, respectively; $P = 0.64$, 0.22 and 0.32, respectively). The SNP adhered to the Hardy–Weinberg expectations ($P > 0.05$).

3.2. Genotype frequencies for rs2156323 SNP in VAV2 and rs2801219 SNP in VAV3

The genotype frequencies for rs2156323 in *VAV2* and rs2801219 in *VAV3* are listed for the POAG, NTG, DG, and control subjects in Table 2. For rs2156323 in *VAV2*, the genotype frequency was not statistically higher in the POAG ($P = 0.25$), the NTG ($P = 0.29$), and the DG ($P = 0.62$) groups than in the control group (Table 2). For rs2801219 in *VAV3*, the genotype frequency was not statistically higher in the POAG ($P = 0.90$), the NTG ($P = 0.07$), and the DG

Table 1
VAV2 and *VAV3* SNPs allele frequencies in patients with POAG, NTG and in controls in Japanese.

SNP	VAV2 (rs2156323 A/G)		*P*-value
Allele	G	A	
POAG ($n = 168$)	0.949	0.051	0.35
NTG ($n = 163$)	0.951	0.049	0.40
DG ($n = 45$)	0.978	0.022	0.51
Control ($n = 180$)	0.964	0.036	
	VAV3 (rs2801219 A/C)		
	A	C	
POAG ($n = 168$)	0.789	0.211	0.64
NTG ($n = 163$)	0.764	0.236	0.22
DG ($n = 45$)	0.756	0.244	0.32
Control ($n = 180$)	0.803	0.197	

The significance of the association was determined by a contingency table analysis using the χ^2 test.